INFLUENCE OF LATERAL-DIRECTIONAL RESPONSES ON FLYING QUALITIES

GORDON R. ENGEL
and
DANIEL W. RICE

27/56

INFLUENCE OF LATERAL-DIRECTIONAL RESPONSES ON FLYING QUALITIES

LCDR. Gordon R. Engel, USN

Lt. Daniel W. Rice, USN

Aeronautical Engineering Department

Report No. 551

May 1961

Submitted in partial fulfillment of the requirements
for the Degree of Master of Science in Engineering
from Princeton University
1961

SUMMARY

A flight test investigation was undertaken at the James Forrestal Research Center, Princeton University, in the spring of 1961 to investigate parameters affecting pilot opinion of airplane lateral-directional flying qualities. In particular, it was desired to study the ratio of the rolling velocity oscillatory envelope amplitude to the "steady state" rolling velocity with an aileron step input imposed upon the system. In order to alter the value of this parameter $C_{n_{\delta a}}$ was varied.

A high performance fighter type aircraft at Mach 1.2 and 35,000 feet was simulated with Princeton's three axis variable stability North American Navion aircraft. The flight simulation was performed over a range of ϕ/β from two to five and dutch roll damping, ζ, from .06 to .13.

Three naval aviators and one civilian pilot were selected from the student body in the Aeronautical Engineering Department of the graduate school to be evaluation pilots for the experiments. Particular attention has been given to the comments of the pilots in an effort to correlate the dynamic responses of the airplane with the opinions of the individual controlling it.

The results of this investigation indicate that the above parameter can be correlated with pilot opinion in predicting handling qualities, when optimum conditions of ϕ/β and ζ exist.

In addition, the size of the β_{DR} oscillations was found to be an important factor affecting pilot opinion of the lateral-directional handling qualities of the aircraft.

ACKNOWLEDGEMENTS

The authors wish to acknowledge the invaluable assistance rendered this project by Professor Edward Seckel of the Princeton University Aeronautical Engineering faculty. In addition, gratitude is expressed to Mr. Enoch Durbin, Mr. Theodor Dukes, and Mr. Gerardus Born of the Flight Mechanics Laboratory for their suggestions and recommendations concerning the autopilot equipment.

The able assistance of Mr. Barry Nixon, Mr. Richard Whitley, Mr. Robert Trauger, Mr. William Szabelski, and Mr. William Bowen in modifying the equipment to meet the requirements of this report is appreciated.

SYMBOLS AND DEFINITIONS

SYMBOLS

d	$\frac{d(\ )}{d(\frac{t}{\tau})}$
β	sideslip angle
β_{DR}	oscillatory envelope amplitude at time zero
δa	aileron deflection; the sum of right and left ailerons
δr	rudder deflection
δr_s	rudder deflection due to lateral stick displacement
Δ	lateral-directional characteristic equation
ζ	damping of the oscillatory (dutch roll) mode
ϕ	roll angle in radians
p, $\dot{\phi}$	roll rate, radians/second
r, $\dot{\psi}$	yaw rate, radians/second
τ	$\frac{m}{\rho S V}$
μ	$\frac{m}{\rho S b}$
C_{y_β}	partial derivative of side force coefficient
C_L	lift coefficient
C_{ℓ_β}	partial derivative of rolling moment coefficient with respect to sideslip angle, β
C_{ℓ_r}	partial derivative of rolling moment coefficient with respect to $\frac{rb}{2V}$
C_{ℓ_p}	partial derivative of rolling moment coefficient with respect to $\frac{pb}{2V}$

J_x	$2(\frac{k_x}{b})^2$
J_z	$2(\frac{k_z}{b})^2$
K_i	feedback gain factor

Dimensional Derivatives

L_p	$\frac{C_{\ell_p}}{2J_x\tau}$	$N_{\delta a}$	$\frac{\mu C_{n_{\delta a}}}{J_z \tau^2}$
L_r	$\frac{C_{\ell_r}}{2J_x\tau}$	Y_v	$\frac{1}{2\tau} C_{y_\beta}$
L_β	$\frac{\mu C_{\ell_\beta}}{J_x \tau^2}$	$N_{\delta r}$	$\frac{\mu C_{n_{\delta r}}}{J_z \tau^2}$
$L_{\delta a}$	$\frac{\mu C_{\ell_{\delta a}}}{J_x \tau^2}$	C_L	$\frac{g}{U_o}$
$L_{\delta r}$	$\frac{\mu C_{\ell_{\delta r}}}{J_x \tau^2}$		
N_p	$\frac{C_{n_p}}{2J_z\tau}$		
N_r	$\frac{C_{n_r}}{2J_z r}$		
N_β	$\frac{\mu C_{n_\beta}}{J_z \tau^2}$		

DEFINITIONS

Double primed derivatives imply aircraft derivatives being simulated by the Navion.

DEFINITIONS

The subscript F following a Roman Numeral such as III_F identifies this point as being a point on the $\frac{\phi}{\beta},\zeta$ plane where a flight evaluation was conducted.

A ratio potentiometer is a pot controlling the gain of a servo drum position feedback signal.

A gain potentiometer is a pot controlling the gain of a feedback signal from a transducer or a signal from one of the electrical flight controls.

Proverse yaw is yaw into the direction of turn.

SECTION I

INTRODUCTION

The lateral-directional flying qualities criteria imposed by the military services, (Reference 1) are suspected of being incomplete in their application to high altitude, high performance manned aircraft. There have been examples in the past of aircraft that were within the current specifications but, nevertheless, fell short of the dynamic qualities that were considered optimum by the pilots who have flown them. Oftentimes in these cases complex and expensive automatic equipment has been installed to modify these undesirable tendencies. This flying qualities investigation has been motivated by the apparent existence of deficiencies in the present criteria.

There have been numerous studies performed in order to pin down a suspected parameter which might adequately describe good or bad handling qualities in the lateral-directional mode. It is recognized that it would be especially useful to find some parameter which, along with others, would aid in the prediction of undesirable flying qualities.

Presently, however, accumulated flight test data is insufficient to permit quantitative evaluations of likely parameters which may be influential in this area. This work is intended, therefore, to supplement and expand existing handling qualities data through examination of a specific parameter not flight tested heretofore.

SECTION II

EQUIPMENT

A North American NAvion airplane equipped for variable stability was used in the flight portion of this investigation. The variable stability was achieved by means of a modified autopilot. Signals from sensing transducers were introduced into the autopilot which deflected the control surfaces in proportion to the measured input. In this manner the system was capable of varying the airplane derivatives. An analog computer was used to assist in the theoretical calculations.

A. Analog Computer and Recorder

A Goodyear Aircraft Corporation Model L3 linear electronic differential analyzer (Reference 2) was used for the analog analysis of this investigation. The computer responses were recorded on a Sanborn Model 150 four channel recorder. The computer and recorder are illustrated in Figure 16.

B. Test Airplane

The NAvion (Figure 1) is an all metal, low wing airplane with retractable tricycle landing gear. A Continental Model E-185 air cooled engine drives a Hartzell variable pitch propeller and is rated at 185 HP for 2300 rpm maximum continuous power at sea level, or 205 HP at 2600 rpm for one minute at take-off. The control surfaces are of conventional design. The frise type ailerons have a streamlined static balance at the outboard lower section of each aileron. Fixed trim tabs are installed on the rudder and right aileron whereas the elevator trim tabs are adjustable from the cockpit. The conventional dual wheel control was removed from the right side and an electric control stick was installed as shown in Figure 3. Electric rudder pedals installed in front of the normal control pedals on the right side were not utilized in this investigation. The control surfaces could be actuated

by either the conventional controls on the left side of the cockpit or when the autopilot was engaged, by the electric controls on the right side. The operation of the electric controls is described with the autopilot equipment. The airplane specifications are listed in Table I.

C. Autopilot

The installation of the variable stability autopilot was performed at Princeton University in 1959-1960 and is described in detail in References 3 and 4.

This autopilot is capable of altering the stability of the NAvion in pitch, roll and yaw and does so through three a.c. summing channels. Figures 5 through 7 describe the summing channels. Into the pitch, roll and yaw channels are fed signals from appropriate transducers, electrical controls, and the trimming system. The difference between the servo drum rotation in each channel and the summation of the input voltages is amplified and causes the servo drum to rotate and position the aircraft control system.

A block diagram of the system showing the gain potentiometers in the yaw and roll channels is included as Figure 8. The quantities can be electrically fed into each channel are:

(1) Roll channel
   a. roll rate
   b. yaw rate
   c. β angle
   d. ϕ angle
   e. aileron stick motion

(2) Yaw channel
   a. roll rate
   b. yaw rate
   c. β angle

(2) Yaw channel

d. lateral stick deflection

e. rudder pedal motion

The electrical controls are located in the right seat of the NAvion and the standard manual controls in the left seat. The gain potentiometer board is situated in an accessible region between the two seats (Figure 4). A terminal board provides flexibility in handling the electrical connections for the autopilot and is mounted over the gyros and amplifiers in the equipment compartment aft of the right seat. It is accessible for maintenance, feedback quantity sign changing, and general trouble shooting. The servo motors themselves are mounted aft of the gyros and amplifiers and are attached to the fuselage frame. Figure 9 illustrates the arrangement of the servo motors and the cabling tie-ins from the motors to the aircraft control system.

During the course of this investigation the position of the tie-ins of the aileron servo cables was changed to that shown in Figure 9 from a previous configuration shown in Reference 4. This change corrected a part of the play that had previously been present in the ailerons.

No feedbacks were utilized in the longitudinal, pitch, channel. The simulation in this study was limited to the lateral-directional mode. Reference 4 describes the longitudinal channel and its capabilities. Elevator control through the electric stick was the only utilization made of the pitch channel servo. This provided the evaluation pilot with longitudinal attitude control.

A number of safety features have been installed in the autopilot system. An electronic cutout will automatically disengage the autopilot should a large error signal appear at the amplifier input. This prevents inadvertent

hard over signals and the possibility of exceeding the "g" tolerances of the airplane. In addition to this, servo clutches were set so that the safety pilot in the left seat was at any time able to override the servo motors in the event that he was unable to disengage the system. Two disengage buttons, one on the electric stick and one to the left of the safety pilot were provided. In addition to these features limit switches were utilized which kept the control motions within selected travel limits consistent with safety and the simulation desired.

The electric control stick had installed within it a spring centering device and fluid dashpots to provide feel for the evaluation pilot. These devices were considered to be inadequate and recommendations covering suggested changes are made later in this report. A small break out force was apparent and was considered objectionable by two of the evaluation pilots. An electrical dead zone of approximately one quarter inch existed at the stick center position and was considered mildly undesirable by most of the evaluation pilots who flew the aircraft. This control is pictured in Figure 3.

D. Special Flight Instrumentation

SFIM Recorder

A SFIM recorder, type A20 was utilized in this study to record one quantity, roll rate. This equipment has its own rate gyro and ratiometer and is independent of the aircraft system except for its 24 volt DC power supply. The SFIM gave a trace on film of the roll rate against time and was used to compare the anticipated results from analog studies with the actual aircraft response.

Sideslip Vane

A Giannini model 2516 sideslip vane is located on the left wingtip approximately four feet ahead of the leading edge. In this position it is relatively clear of the local flow fields. The effect of the yawing velocity

due to vane offset from the c.g. was computed and considered in Appendix D. The vane has two potentiometers within it which allows this quantity to be fed into both the yaw and roll channels. The mounting for this vane has been stiffened to prevent vibrations induced by the aircraft motions from affecting the β feedback. However, in those aircraft motions which resulted in large yawing oscillations some high frequency vibration of the entire sideslip mounting was in evidence which is thought to have been a minor factor in reducing the simulation reliability.

An angle of attack vane was mounted on the same structure as the sideslip vane but was not used in this lateral study. Figure 2 shows the sideslip vane.

Rate Gyros

Minneapolis Honeywell model JG 7003A-11 rate gyros are installed in this autopilot. They receive power from a 400 cycle, 115 volt, autopilot inverter installed in the equipment compartment.

The specifications of the autopilot and special instrumentation are enumerated in detail in References 3 and 4.

SECTION III

DISCUSSION

A. Theoretical Analysis

The development of a criterion by which the lateral-directional mode of the aircraft may be evaluated has become, with the advent of the high performance aircraft, an important area of investigation. The specific area of study embodied in this report is that of investigating the roll response due to aileron deflection of a high performance aircraft at high Mach number and altitude. Rudder pedal inputs were not utilized in this analysis. The flight regime under investigation is of obvious importance to the fighter aircraft attempting to track and fire upon a fast, evasive target.

It is felt that the pilot undertaking the roll maneuvers required in this task would desire a roll rate proportional to his aileron deflection and a response as free as possible from time lags and transient oscillations. It would be useful then to have a parameter or several parameters which would be a measure of the departure of the roll response from the ideal, and in addition which could correctly and easily reflect pilot opinion in terms of physical quantities which can be measured by examination of roll rate time histories.

If the airplane designer could then interpret the chosen parameters in terms of stability derivatives it is conceivable that he could, in the aircraft design phases, build into it qualities which would ensure optimum dynamic performance and thereby alleviate any need for future modifications which are inevitably costly in time and dollars.

It is the purpose of this report to flight test a specific parameter which has the aforementioned advantages of simplicity, and which is easily

seen on the lateral-directional time history traces, and furthermore, appears to have a direct physical bearing on the motion that the pilot feels as the rolling mode of the aircraft proceeds. This parameter is defined as the magnitude of the oscillatory envelope of the rolling velocity at time zero divided by the essentially "steady state" roll rate with a step input imposed on the system. This so called "steady state" component may build or decay w ith a long time constant depending upon whether the spiral mode is unstable or stable. The parameter will be referred to henceforth as K_3/K_1 throughout this report.

Pictured here is a representation of the parameter under discussion:

Roll rate due to step input

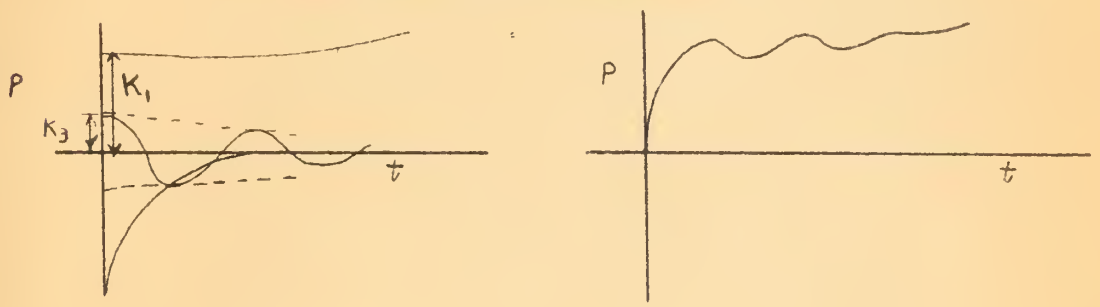

$$p = K_1 e^{\frac{1}{T_s}t} + K_2 e^{\frac{1}{T_R}t} + K_3 e^{\zeta\omega t} \cos(\omega t + \eta)$$

The linear lateral-directional equations of motion with an aileron input obtained from Reference 5 and used in this study are:

$$(C_{y_\beta} - 2d)\beta - 2d\psi + C_L\phi = 0$$

$$\mu C_{\ell_\beta}\beta + \frac{C_{\ell_r}}{2} d\psi + (\frac{C_{\ell_p}}{2} d - J_x d^2)\phi = - \mu C_{\ell_{\delta a}} \delta a$$

$$\mu C_{n_\beta}\beta + (\frac{C_{n_r}}{2} - J_z d)d\psi + \frac{C_{n_p}}{2} d\phi = - \mu C_{n_{\delta a}} \delta a$$

Products of inertia were neglected in this study. For the class of fighter considered Reference 6 indicates I_{xz} 10% of I_x and 1% of I_z. In addition to the above the XZ plane was considered a plane of symmetry.

Approximate derivatives for a fighter airplane at M = 1.2 and at 35,000 feet altitude were taken from NASA reports and utilized as a starting point from which they were varied in order to achieve a range of $\frac{\phi}{\beta}$ from .3 to 10 and a range of ζ_{DR} from .1 to .3. This was considered to be a broad range of these parameters within which pilot opinion studies were to be conducted in Princeton University's variable stability North American NAvion airplane.

In order to achieve this variation in $\frac{\phi}{\beta}$ and ζ it was initially decided to vary the following derivatives in the characteristic equation: Cn_r, $C\ell_\beta$, Cn_p, and Cn_β. Root loci were drawn with these derivatives as variables, primarily to detect their effect on dutch roll damping and the roots of the characteristic equation. Figures 10 through 13 depict these root loci.

Cn_r was shown to be the determining factor in the variation of ζ_{DR} whereas the other derivatives that were varied had but a small effect on dutch roll damping. In order to detect the effect on $\frac{\phi}{\beta}$ of the four variable derivatives a combined analog and analytical approach was utilized. $C\ell_\beta$ and Cn_β were determined to be the derivatives which most influenced $\frac{\phi}{\beta}$. High $C\ell_\beta$ (negative) and low Cn_β resulted in high $\frac{\phi}{p}$. This can readily be shown by analog treatment and is also apparent when viewing this combination of derivatives from the standpoint of what physically happens to an airplane subjected to a small disturbance. Appendix A details the analytical approach to this examination.

Figure 14 shows a plot of ten points on a plane of $\frac{\phi}{\beta}$ vs. ζ. Each point represents a specific set of stability derivatives and a resulting characteristic equation. The stability derivatives corresponding to each point are listed in Table II.

The roll time constant for each point examined was approximately .25 seconds and the spiral mode time constant ranged from a very large value in the unstable regime to a stable spiral time constant of 7.2 seconds.

It should be noted that values of the various derivatives used to establish points I through X on the $\frac{\phi}{\beta}, \zeta$ plane may not be in every case attainable in the basic design of a fighter aircraft. However, with the aid of artificial damping the large Cn_r's, for example, could be achieved. None of the values of derivatives listed in Table II concerning points I through X are thought to be unrealistic.

This spectrum of points when examined in the analog study gave a broad base for examination of the rolling velocity traces and their variation as the proposed parameter, K_3/K_1, was varied.

In order to vary K_3/K_1 the yawing moment due to aileron displacement, $Cn_{\zeta a}$, was varied through both positive and negative values with a selected value of $C\ell_{\zeta a}$ of + .04. This value was representative of the class airplane being studied at M = 1.2 and 35,000 feet, (Reference 6).

Values of $Cn_{\zeta a}$ in adverse yaw were varied from zero to - .0343 and in proverse yaw from zero to + .03. Exceptions were made to these limits on the analog in cases where values of adverse $Cn_{\zeta a}$ up to - .0343 did not produce a detectable change in K_3/K_1. However, - .0343 represents a large value in relation to the $C\ell_{\zeta a}$ being used as indicated in Reference 6, where a member of the class fighter being examined is shown with a maximum $Cn_{\zeta a}$ being only 50% of $C\ell_{\zeta a}$.

Some values of the parameter, K_3/K_1, were computed both analytically and by the analog computer. The computer study was particularly adaptable for examining K_3/K_1 as $Cn_{\zeta a}$ was varied. An interesting point was seen as these numerical values were found. It appears that for the low $\frac{\phi}{\beta}$ ranges

(below .7) $Cn_{\delta a}$ must be two to three times $C\ell_{\delta a}$ in order to give any discernible magnitude to the parameter K_3/K_1. This finding would indicate that ordinarily with low $\frac{\phi}{\beta}$ aircraft it is unlikely that sufficient adverse yaw due to aileron displacement would be present at any time to cause a problem area noticeable to the pilot insofar as roll rate transient oscillations were concerned. However, from available data, it appears that the aircraft under consideration, the high performance fighter, is in a $\frac{\phi}{\beta}$ range greater than one, and in this range adverse yaw due to aileron deflection has a marked effect on the size of the suggested parameter. As the adverse yaw increased in value, roll rate reversal was noted in several cases. This was relatively easily achieved with small values of adverse yaw in the higher $\frac{\phi}{\beta}$ region, above five. A further treatment of this subject will be given in the ensuing discussion covering the analog computer study.

In view of the possibility in some current aircraft of having ailerons positioned quite near the vertical tail, it becomes of practical interest to think not only in terms of adverse yaw, but in addition to consider proverse yaw, that is, yaw into the turn. Pressure fields may be created in the instance mentioned where the aircraft will be yawed with the turn. For this reason the analytical and flight studies were extended beyond adverse yaw to include proverse yaw, and the parameter, K_3/K_1, was found to experience little variation as $Cn_{\delta a}$ increased from zero to positive values. This feature is clearly pointed out in the analog study. It is obvious that the magnitude of the transient oscillations increases in proverse as well as in adverse yaw. However, coincident with this is an increase in the value of the roll rate itself, which in turn prevents any appreciable increase in K_3/K_1 through a range of proverse $Cn_{\delta a}$. Figure 18 shows a plot of the values of K_3/K_1 for both adverse and proverse yaw at each stability derivative configuration being examined.

An exact simulation of the study described, heretofore, would have been desirable on the NAvion aircraft, however, due to equipment limitations it was not possible to simulate exactly the specific $\frac{\phi}{\beta}, \zeta$ points I through X that were examined theoretically and by analog. A further investigation was conducted of the compromises that would have to be made in order to achieve the desired pilot opinion study in the NAvion.

The variable stability equipment in the NAvion is not capable of varying the terms in the side force equation, that is, C_L and C_{Y_β}. The side force equation terms of points I through X were therefore not able to be simulated in the NAvion exactly. In order to determine the effect on dynamic response of having to accept the C_{Y_β} and C_L of the NAvion an analog study was run and it was determined that the only term of the two which had a significant effect in changing the dynamic response was the C_L term. The principal effect of operating at the C_L of the NAvion, .5, instead of that of the high performance aircraft was to reduce the dutch roll damping.

An analog computer study, Figure 19, is included in the report which pictures the roll response anticipated in the NAvion as it performed the simulation. The derivative values used in this analog study, as will be mentioned in detail under the analog section of the report, were precisely the same as those used to examine points I through X described previously except that the C_L of the NAvion, .5, was used rather than the C_L of .1 more typical of the high performance fighter.

B. Analog Computer Study

Procedures

The analog computer study was performed to expand the results of the theoretical investigation. Having determined the derivative values for the

desired $\frac{\phi}{\beta}$ and ζ_{DR} points, Table II, it was next necessary to obtain the ratios of K_3/K_1 as $Cn_{\delta a}$ varied over the desired range of proverse and adverse aileron yaw (+ .03 to - .0343) as established by the limits of the gain in the test airplane's variable stability system.

The linearized non-dimensional equations of motion were determined as described in Appendix B. These equations were set up on the GEDA computer (Figures 16 and 17) and recordings of the roll rate and sideslip transient responses for various values of $Cn_{\delta a}$ at each point were plotted by the Sanborn Recorder. Recorder scales were selected to give large amplitudes in order to observe the oscillation characteristics. The time scale was set at 10 mm per second in order to obtain accurate measurements of the period and time to damp to half amplitude. In addition, the large amplitude and moderately high speed provided optimum conditions to extrapolate the observed response to obtain the values of K_3 and K_1 at time zero. The previously calculated damping ratios were verified from the analog data by the expression:

$$\zeta_{DR} = \frac{.693}{T_{1/2}}\,\omega$$

where $$\omega = \frac{2\Pi}{P}$$

The ζ_{DR} values could also be readily obtained using Figure A4 of Reference 7. The analog recordings for the ten points of the theoretical investigation are presented in Figure 18. In order to apply the results of the theoretical investigation to the NAvion variable stability system, it was necessary to consider the lift coefficient of the NAvion (C_L = 0.5) rather than the previously established lift coefficient (C_L = 0.1) for the high performance airplane. Therefore, an analog computer study for the flight test evaluation was performed using the same derivatives as in the initial investigation except that the C_L

in the sideforce equation was set equal to 0.5. This change was accomplished by changing the R_4 resistance (Figure 17) from 1 MΩ to 0.2 MΩ which increased the gain of amplifier 4 by a factor of five. The points of the analog study corresponding to the flight test evaluation are labeled with a subscript "F" i.e., POINT III_F, etc., as described in Table III.

Analysis of Computer Study

The results of the analog computer study are illustrated in Figures 18 and 19. Figure 18 describes the roll-rate and sideslip responses of the theoretical study high performance airplane (C_L = 0.1) and Figure 19 describes the responses corresponding to the flight test evaluation (C_L = 0.5). In comparing the two sets of data it is noted that the primary difference appears to be in the reduced damping ratio (ζ_{DR}) for the higher C_L responses. That is, instead of damping ratios of approximately 0.1 and 0.3, the increased C_L resulted in corresponding damping ratios of approximately 0.06 and 0.13. If one considers a plot of the dutch roll stability boundary in the μCn_β, $\mu C\ell_\beta$ plane (Reference 5), the effect of increased C_L is to move the oscillatory boundary to the left and reduce the stability, ζ_{DR}, as is herein observed.

Certain characteristics are common to the responses of all ten points in the theoretical investigation (Figure 18). As $Cn_{\zeta a}$ varies from the proverse condition (+ $Cn_{\zeta a}$) to the adverse condition (- $Cn_{\zeta a}$), the "steady state" roll rate, K_1, decreases. In flight this decrease would have the effect of reducing the control sensitivity and maximum roll rate. For $Cn_{\zeta a}$ = 0, the "steady state" roll rate due to a 10 degree aileron step input is relatively constant at between 60 and 70 degrees per second for all ten points. It is also noted that the magnitudes of both the roll-rate and the sideslip oscillations increase as $Cn_{\zeta a}$ increases in both proverse and adverse yaw. It is this characteristic which indicates that the pilot opinion of lateral flying qualities might be

a function of the ratio of the amplitude of the dutch roll oscillation to the "steady state" roll-rate. The amplitude of the roll-rate oscillations is a function of $\frac{\phi}{\beta}$, the greatest amplitudes occurring at the highest $\frac{\phi}{\beta}$ points and almost no apparent roll oscillations occurring at the lowest $\frac{\phi}{\beta}$ points. This characteristic is true for both the proverse and the adverse yaw conditions. In the high $\frac{\phi}{\beta}$ adverse yaw conditions the roll-rate amplitude is great enough to cause roll reversal. It is noted that the amplitude of the sideslip oscillations, though decreasing slightly with decreasing $\frac{\phi}{\beta}$, are clearly present at the lowest $\frac{\phi}{\beta}$ points.

C. Flight Test Evaluation

1.Simulation Procedures

In order to perform a simulation of the proposed high performance aircraft in the NAvion the equations of motion were dimensionalized as described in Appendix C, resulting in the following equations in real time:

$$(Y_v - s)\beta - \dot{\psi} + \frac{g}{U_o}\phi = 0$$

$$L_\beta\beta + L_r\dot{\psi} + (L_p s - s^2)\phi = -L_{\delta a}\delta a$$

$$N_\beta\beta + (N_r - s)\dot{\psi} + N_p s\phi = -N_{\delta a}\delta a$$

The derivatives of the NAvion were obtained from Reference 8. With these dimensionalized derivatives (Table IV), and the computed dimensionalized derivatives of the airplane being simulated, it was possible, using procedures established in Reference 3, to determine the feedback gains necessary to give the NAvion the dynamic characteristics of the simulated airplane. The gains computed were then controlled at the potentiometer panel in the NAvion.

An example of the procudure used to calculate the gain constants required to simulate the high performance airplane is described by the following pair of simultaneous equations where the double primed values represent the quantities being simulated and the unprimed quantities, the basic NAvion:

$$L_\beta'' = L_\beta + K_4 L_{\delta r} + K_8 L_{\delta a}$$

$$N_\beta'' = N_\beta + K_4 N_{\delta r} + K_8 N_{\delta a}$$

The gain constants K_4 and K_8 become:

$$K_4 = \frac{(L_\beta'' - L_\beta) N_{\delta a} - (N_\beta'' - N_\beta) L_{\delta a}}{L_{\delta r} N_{\delta a} - N_{\delta r} L_{\delta a}}$$

$$K_8 = \frac{(N_\beta'' - N_\beta) L_{\delta r} - (L_\beta'' - L_\beta) N_{\delta r}}{L_{\delta r} N_{\delta a} - N_{\delta r} L_{\delta a}}$$

All of the defining equations concerned are listed in Table V along with definitions of the various gain constants.

Simplified equations for the gain constants are listed in Table VI.

After determining the values of the gain constants for the simulation desired, the aircraft system was calibrated in order to determine whether these gains could be attained.

It is pointed out here that the provision for roll angle feedback into the roll channel was not used in this study. However, all the other feedbacks shown in Figure 8 and listed previously were utilized.

Rate gyros were calibrated on a specially constructed table which rotated at a controllable rate. For various rates of turn of the calibration table the rate gyros, electrically connected with the aircraft system, gave a displacement to the control surfaces which was measured by protractor for a range of gain potentiometer settings.

The sideslip vane calibrations were conducted by moving the vane through a specified angle measured by a protractor and then measuring the control surface deflections at different gain potentiometer settings.

From the above procedures, calibration curves of degrees rudder per degree sideslip vane, degrees aileron per degree per second $\dot{\phi}$, etc. were plotted against potentiometer face plate settings. These calibration curves are shown in Figures 20 through 26.

There exist limitations inherent in the autopilot design on the values of feedback gain attainable. It was discovered that through adjustment of amplifier gains to the highest permissible values, increase of potentiometer voltages, and reduction of ratio potentiometer settings, that the sought after simulation could be realized. The best range of simulation lay between $\frac{\phi}{\beta}$ of approximately two and five. The reduction in ratio pot settings necessary to achieve high gains resulted in large peck sizes and increased time lags in the autopilot servos. Some loss in reliability was recognized as accompanying the reduced ratio pot settings.

It was not possible without extensive changes in the autopilot circuitry to achieve a realistic simulation in the very low $\frac{\phi}{\beta}$ region due to large unattainable values of K_4 gain (rudder deflection per degree β). This high K_4 was necessary due to the high μ and C_{n_β} conditions being simulated.

Some divergent oscillations in yaw were encountered when trying to flight test the very low $\frac{\phi}{\beta}$ areas that were not anticipated from analog study and were probably due to lags in the autopilot.

In the high $\frac{\phi}{\beta}$ range, above 8, the high $C\ell_\beta$ combined with high μ resulted in unattainable values of K_8 (aileron deflection per degree β). The single factor that is most responsible for both of these problems is the high μ value which enters into the dimensionalized derivatives in such a way as to render the feedback values for low $\frac{\phi}{\beta}$ and high $\frac{\phi}{\beta}$ difficult to attain.

It is pointed out here that the very low $\frac{\phi}{\beta}$ simulation, below .7, was also made impractical by the fact that insufficient adverse yaw was available through the autopilot, that is, degrees rudder per inch of lateral stick deflection to appreciably effect the parameter being investigated, K_3/K_1. It was pointed out previously that extremely large values of adverse yaw were required at low $\frac{\phi}{\beta}$ to have any effect of the size of K_3/K_1.

In addition to the problem areas mentioned above another difficulty which arose was the necessity of using some very small gain values which resulted in very small gain pot face settings. Vernier type potentiometers would have increased the repeatibility of results. With sufficient care in calibration, however, and subsequent careful setting of potentiometers prior to actual testing it was felt that this problem was handled with a minimum loss of reliability.

The other major problem spot in trying to achieve good simulation occurs in the area of cable stretch and pulley bending. The aileron cable stretch problem was partially solved by routing the aileron servo cables as shown in Figure 9 in order to relieve system slack. This change was discussed in the equipment section. The rudder control cables appear to be free from excessive yield that could influence flight results, however there is still a small amount of play in the aileron. Mounting the servo potentiometer in the wing where it would measure actual aileron travel would be a solution to this problem.

No feedbacks were employed in the longitudinal system. The elevator gain potentiometer was adjusted to a value which gave a comfortable longitudinal response to the evaluation pilots. The longitudinal characteristics were satisfactory throughout the testing.

Despite the difficulties mentioned heretofore the simulation achieved on the flights in the mid $\frac{\phi}{\beta}$ range, two to five, is felt to have been reasonably well attained. Results of SFIM recorder roll rate traces of flight points III_F, IV_F, V_F and VI_F indicated agreement with computer predicted results in this area.

2. Flight Procedures

Method of Test

The principal objective of the flight test evaluation was to determine whether or not the parameter K_3/K_1 could be used to measure pilot opinion of

the lateral-directional flying qualities of a high performance airplane. Various points defined by their ratio of dutch roll $\frac{\phi}{\beta}$ and ζ_{DR} were investigated over a range of $\pm$ $Cn_{\delta a}$. A secondary purpose was to observe other parameters which might also measure these flying qualities. Because the flight investigation was primarily concerned with the airplane's response to aileron deflection, the evaluation pilot had no rudder control. Rudder positions were established by the variable feedback system only.

The flight tests were performed in a cruise configuration (Reference 1) at a density altitude of 6500 feet and a true airspeed of 120 mph. With these conditions and an average gross weight of approximately 2750 pounds, the NAvion lift coefficient was calculated to be 0.5. All tests were initiated from a steady, level flight condition.

In order to measure the lateral-directional flying qualities of the airplane as an operational vehicle, it was decided that two types of maneuvers should be investigated; (1) the shallow turn associated with instrument or navigation flying, (2) the steep turn associated with the tracking of an evasive target.

For the shallow turn maneuver, the evaluation pilot was instructed to roll the airplane to a 10° to 20° bank angle, to perform a steady turn of 15 to 30 degrees, and to return to level flight. The quality of the maneuver was measured by the ease and comfort and the precision with which the pilot could perform the maneuver. These items were measured by: (1) the initial roll response to control stick displacement, (2) the smoothness of the roll-rate, (3) the ability of the pilot to stop at his desired bank angle, (4) the ability to hold a steady shallow bank, (5) the pilot's ability to return to and maintain steady level flight.

The evaluation pilot was then instructed to perform a rapid roll to between 30° and 45°, to track the horizon for a turn of approximately 45°, and return rapidly to steady level flight. The pilot's opinion of the lateral-directional response for an abrupt steep turn was determined essentially by the same items as for the shallow turn except that particular attention was given to observing the ability to maintain a steady rate of turn around the horizon. This corresponded to the quality of the airplane in tracking a target.

To insure that each test condition would be graded on its own merits and not compared with preceding runs, the test conditions were selected at random and were occasionally repeated to check the consistency of the pilot in his grading. Because of the amount of electrical rework required to change from adverse yaw simulation to the proverse simulation, all tests in the former condition were performed prior to the evaluation of the latter.

The evaluation pilot was asked to qualify each of his opinion grades. His comments were recorded by the check pilot on an evaluation sheet. Each of the four evaluation pilots flew all of the 32 adverse and proverse yaw test conditions described by the analog study of Figure 19.

Two flights of approximately one hour duration per flight were performed by each pilot. It is of interest to note that mildly turbulent weather had a marked effect in lowering the pilots' opinions of the flight test runs.

Pilot Opinion

Pilot opinions of the lateral flying qualities were obtained by four experienced pilots, one a civilian and three naval aviators. A description of pilot experience is shown in Table VII.

In order to establish a somewhat standard rating scale, References 9 through 12 were reviewed and a composite opinion scale (Table VIII) was established keeping in mind that the principal responses being evaluated

were in roll and yaw. In general, the evaluation pilot would give the maneuver an adjective grade of good, satisfactory, unsatisfactory, or unflyable with plus and minus designations where appropriate. These adjective grades were later converted to the numerical system for convenience of plotting.

The rating of "good" inferred that the airplane responded well with, at the most, only mildly unpleasant characteristics which would not adversely effect its primary mission as a target tracking vehicle. "Satisfactory" implied that the airplane had moderately unpleasant characteristics but a fair chance of accomplishing its mission and therefore was marginally acceptable. "Unsatisfactory" indicated that the airplane was flyable but difficult to handle because of poorly damped oscillatory motions or extremely high control sensitivity. "Unflyable" meant that the airplane became uncontrollable.

3. Analysis of Flight Test Results

The results of the flight test evaluation are presented in Figures 27 through 31. Figure 27 is a plot of K_3/K_1 vs $Cn_{,a}$ for the high performance airplane of the theoretical investigation and Figure 28 is a corresponding plot of K_3/K_1 for the flight test evaluation. The variable $Cn_{,a}$ for the four flight test points (III_F - VI_F) is plotted against pilot opinion in Figure 29. Figure 30 correlates the data from Figures 28 and 29 to obtain a plot of K_3/K_1 vs Pilot Opinion. Inasmuch as one of the objections was the excessive β oscillation, Pilot Opinion vs β is described in Figure 31.

A preliminary flight investigation in the adverse aileron yaw condition was conducted for the ten points with dutch roll $\frac{\phi}{\beta}$ ranging from approximately 10 to 0.3 and ζ_{DR} of approximately .06 and .13. It was determined that for $\frac{\phi}{\beta} \geq 8$ and for $\frac{\phi}{\beta} \leq 0.7$ that the flying qualities were unsatisfactory due to excessive lateral directional oscillations. Therefore the flight evaluation was concentrated on points III_F through VI_F where $\frac{\phi}{\beta} \doteq 5$ and 2. From NASA data it was observed that supersonic fighter airplanes do operate in this range.

In order to analyze the pilot opinion systematically, the ten points will first be evaluated individually. Following this, the overall evaluation will be summarized with a view toward establishing the relationship between pilot opinion of the lateral flying qualities and a parameter which the pilot senses and that will measure his opinion over a reasonable range of $\frac{\phi}{\beta}$ and ζ conditions.

Point I_F(ϕ/β = 8.1, $\zeta \doteq .06$)
and
Point II_F(ϕ/β = 9.5, $\zeta \doteq .13$)

Points I_F and II_F were tested in the preliminary flight investigation and considered to be "unsatisfactory" primarily due to high amplitude, weakly damped combined rolling and yawing (dutch roll) oscillations which were easily excited by small lateral control stick motions. As the aileron adverse yaw ($- Cn_{\xi a}$) was increased, roll-rate oscillations became more objectionable and lowered the pilot's opinion of the flying qualities. The increased damping ($\zeta_{DR} \doteq 0.13$) for Point II_F decreased the magnitude of the combined rolling and yawing oscillations. However, the flying qualities were still "unsatisfactory" and decreased with increasing aileron adverse yaw again because of the increased magnitude of the roll-rate oscillations.

These high ϕ/β flight conditions required that 5 degrees of aileron be provided by the autopilot servo for each one degree of sideslip. This relatively large aileron angle requirement is difficult to achieve rapidly with the servo system used in this investigation. The time lag apparently reduced the already low ζ_{DR} programmed into the simulation and caused the low damping of the dutch roll oscillations in flight.

Some of the pilots began to feel ill within five minutes of flying because of the high magnitude and weak damping of the dutch roll oscillations.

Point III_F ($\phi/\beta = .5.3$, $\zeta \doteq .06$)

Point III_F with its lower ϕ/β furnished slightly improved flying qualities over the higher ϕ/β points and pilot opinion ranged from "unsatisfactory-plus" at $Cn_{\delta a} = 0$ to "unsatisfactory-minus" at high $\pm Cn_{\zeta a}$.

For $Cn_{\zeta a} = 0$ the pilots objected to the moderate magnitude and low damping of the combined rolling and yawing (dutch roll) oscillations which were easily excited even by small lateral stick displacements.

As aileron adverse yaw ($- Cn_{\zeta a}$) was increased, the dutch roll oscillation remained of moderate magnitude but the roll rate oscillations made it difficult to maintain a steady bank angle and thereby lowered the pilot's opinion of the flying qualities. Some of the pilots felt that the increased aileron adverse yaw had a damping effect on the dutch-roll oscillations and thereby tended to improve the flying qualities. This feeling of improved damping might come from the reduced magnitude of the "steady state" response and resulting decrease in control stick sensitivity with increases in $- Cn_{\delta a}$ as may be observed in Figure 19 (Point III_F). This phenomena is also discussed in References 11 and 13 regarding the effects of pilot induced oscillations which occur with low ζ_{DR}.

As aileron proverse yaw ($+ Cn_{\zeta a}$) was increased, the magnitude of the combined rolling and yawing oscillations increased and the damping appeared to decrease. The latter effect might be attributed to the decreased damping associated with the servo system lags where servo responses of high magnitude are required. This deficiency has been previously described in Points I_F and II_F. No objections were made to roll-rate oscillations in the Point III_F proverse yaw investigation. The lack of any objections might be expected because of two conditions. First, the combined rolling and yawing oscillations were of such a magnitude as to almost mask any roll-rate variations. Second,

from Figure 19 (Point III_F) and from Figure 28, it is observed that the ratio of the magnitude of the roll-rate oscillation to "steady state" input increases slowly for increases in proverse yaw.

Point IV_F(ϕ/β = 5.6, $\zeta \doteq 0.13$)

The increase in damping gave Point IV_F a rating of "satisfactory-plus" at $Cn_{\zeta a}$= 0, "satisfactory" at low $\pm Cn_{\zeta a}$, and "unsatisfactory" for high $\pm Cn_{\zeta a}$ with pilot opinion of the lateral flying qualities decreasing more rapidly in the proverse than in the adverse condition.

For $Cn_{\delta a}$ = 0 the pilots noted a slight low frequency yawing oscillation which was excited by lateral stick movements. This yawing condition was only mildly objectionable.

As aileron adverse yaw was applied, a combined rolling and yawing (dutch roll) osoillation and a variation in roll-rate appeared in response to lateral stick displacements. For high aileron adverse yaw ($Cn_{\zeta a}$ = - .0343) the combined rolling and yawing (dutch roll) oscillations and the uneven roll-rate with roll reversal tendencies (airplane tendency to reverse in direction of roll) appeared to have equal weights in lowering the pilot opinion to "unsatisfactory."

When the aileron proverse yaw was increased the pilots objected to the noticeable increase in control stick sensitivity. That is, the "steady state" roll rate per unit of stick displacement was increased. This effect can be observed in Figure 19 (Point IV_F). No attempt was made in the calculations to maintain a constant "steady state" roll rate. As in the aileron adverse yaw condition, any lateral stick motion excited a combined rolling and yawing oscillation which increased in magnitude with increases in aileron proverse

yaw. At $Cn_{\zeta a}$ = + .03 the control stick sensitivity and the combined rolling and yawing oscillations excited by stick movements appeared to have equal weights in causing the pilot opinion to become "unsatisfactory."

Point V_F(ϕ/β = 1.9, $\zeta \doteq$ .06)

This point was rated "unsatisfactory" primarily because of yawing oscillations which were neutrally damped except at high aileron proverse yaw where the yawing oscillations were divergent.

At $Cn_{\zeta a}$ = 0 any lateral stick movements excited yawing oscillations of moderate magnitude and neutral damping.

As aileron adverse yaw (- $Cn_{\zeta a}$) was increased, it appeared to some pilots that the magnitude of the yawing oscillations was reduced, thereby tending to improve the flying qualities. The apparent improvement in pilot opinion might have resulted from reduced lateral stick sensitivity as observed by the reduced "steady state" roll rate in Figure 19. At $Cn_{\delta a}$ = - .0343 the magnitude of the roll-rate oscillations became the predominant factor in lowering pilot opinion.

For increases in aileron proverse yaw (+ $Cn_{\delta a}$) the yawing oscillations increased in magnitude and at $Cn_{\delta a}$ = + .03, the yawing oscillations became divergent. The pilots commented that the initial roll response was "good" but that the resulting yawing oscillation was "unsatisfactory."

Point VI_F(ϕ/β = 2.0, $\zeta \doteq$ .13)

The pilot opinions for this point were the highest of the points investigated. Except at high $\pm$ $Cn_{\zeta a}$, the ratings were "satisfactory" or better.

At $Cn_{\zeta_a} = 0$ the only adverse comments referred to the deficiencies in the construction of the electric control stick. These consisted of a 1/4 inch dead-zone at the stick center position, a small but apparently excessive break-out force for initial lateral stick displacements, and a very small control force gradient. The control stick was a package unit and because of time limitations, it was decided not to attempt to alter the deficiencies. The evaluation pilots were advised of the control stick problems and requested to attempt to disregard same in forming their flying quality opinions.

As aileron adverse yaw was increased, roll-rate oscillations became more noticeable until at $Cn_{\zeta_a} = -.0343$ the roll-rate was so unsteady that the flying quality was considered "unsatisfactory."

For increases in aileron proverse yaw, the pilots noted an increased stick sensitivity, a light yawing oscillation, and a rolling oscillation which the pilot himself appeared to have a destabilizing effect on. It is felt that the last phenomena may be the result of the first wherein it would be difficult to make a small exact bank angle change with a highly sensitive control stick. The tendency would be to over-shoot the desired bank angle. Then any applied control stick corrections combined with the human pilot's inherent reaction lags could have destabilizing effects on the rolling motions of the aircraft.

Points VII_F - $X_F(\phi/\beta \doteq .3$ and $.7$, $\zeta_{DR} \doteq .06$ and $.13)$

These points were investigated in the preliminary flight evaluation and all resulted in divergent yawing oscillations as soon as any aircraft disturbance occurred. Increasing the ζ_{DR} from 0.6 to .13 increased the time of oscillation build-up and thereby tended to improve the flying qualities, but the divergence remained and the conditions were still "unflyable." Had the pilot or servo limit automatic cutouts not been present, the forces might

have damaged the aircraft structure. In view of the fact that the sideslip feedback to the rudder was 3^{o} or per $1^{o}\beta$, the rudder servo was required to make large oscillatory movements of the rudder surface in half cycles of one second duration (Period = 2 seconds). This is apparently more than can be expected of the present installation and the lag of the servo system was great enough to cause instability even with a programmed dutch roll damping ratio of 0.13.

Because of the relatively long period of the yawing oscillations, approximately 2 seconds, the pilots felt that some control might have been maintained if they had been able to use the rudder pedals. As previously stated, it was the intention of this investigation to evaluate the airplane response to aileron displacement only and to prevent the pilot from affecting the motion through the use of rudders.

Summary of Flight Analysis

Point VI_F with $\phi/\beta \doteq 2$ and $\zeta_{DR} \doteq .13$ was rated "good", the highest pilot opinion rating given for the points investigated. Point IV_F with $\phi/\beta \doteq 5$ and $\zeta_{DR} \doteq .13$ was considered to be the next best point, but combined rolling and yawing oscillations and control stick sensitivity prevented more than a "satisfactory" rating. Point III_F with weakly damped rolling and yawing oscillations was considered to be better than Point V_F primarily because of the pilot's strong objection to yawing oscillations which were predominant in the latter point. Points I_F and II_F were "unsatisfactory" because of the weakly damped combined rolling and yawing oscillations, and Points VII_F through X_F were "unflyable" with divergent yawing oscillations.

In the present investigation the pilot opinion was highest for $\phi/\beta \doteq 2$. In similar tests described in Reference 9 where the data is given in terms of ϕ/n_e and $1/C_{l_{1/2}}$, the highest pilot opinion corresponded to a ϕ/β range of

approximately 2.5 to 4.5. In Reference 11 the pilots show a preference for ϕ/β between 2.5 and 3.5 and low pilot opinion for $\phi/\beta > 5$ with $\zeta_{DR} \doteq .1$. This indicates that there may be a small range of ϕ/β values for which high performance aircraft will have optimum lateral flying qualities. It is of interest to note that Reference 9 concluded that the maximum tolerable $\phi/\beta \doteq 7.5$ and that Reference 11 shows that for $\zeta_{DR} \doteq .4$, pilot opinions have an adjective rating of "good" for ϕ/β as high as 7.

It is apparent that there is a minimum value of dutch roll damping required for acceptable lateral oscillatory characteristics of high performance fighter airplanes. The results of this investigation show the minimum ζ_{DR} to be approximately 0.1 for oscillatory ϕ/β values in the range of 2 to 5. It is noted that the Military Specifications, Reference 1, require increased dutch roll damping $(1/C_{1/2})$ for higher values of ϕ/v_e. A requirement for this increase in ζ_{DR} may be observed in Figure 30 where the pilot opinion of Point IV_F is lower than that for Point VI_F. Both points have the same $\zeta_{DR} \doteq .13$, but Point IV_F has the higher $\phi/\beta \doteq 5$.

In the aileron proverse yaw investigations one of the principal pilot objections was in regard to increased control stick sensitivity. This increased sensitivity is considered to be partially caused by the higher "steady state" roll rate associated with proverse yaw. However, it is considered probable that the control stick deficiencies including a large stick center dead-zone and a large break-out force followed by a low force gradient per stick displacement, also contributed to the apparent control sensitivity.

Curves of K_3/K_1 versus pilot opinion are plotted in Figure 30 for the various flight test values of ϕ/β and ζ_{DR}. The crossing of the various curves would indicate that K_3/K_1 is not a valid general parameter for measuring lateral

flying qualities. It appears to be extremely dependent upon ϕ/β and ζ_{DR}. The flight investigation encompassed a region of unsatisfactory to marginally acceptable dutch roll damping in which only one point was rated as having "good" flying qualities. It was in the flight evaluation of this "good" point that the pilots principal objection was the magnitude of the roll rate oscillation. Therefore, it seems that the K_3/K_1 parameter might be valid for measuring lateral flying qualities, providing there is sufficient ζ_{DR} to eliminate the type of oscillations which predominate for the region of ϕ/β concerned.

Because the pilots objected in many instances, especially in the low ϕ/β investigation, to the yawing oscillations, curves of the dutch roll β vs Pilot Opinion were plotted in Figure 31. The magnitude of the β oscillations was measured from the analog computer recordings in Figure 19. It is interesting to note that the curves do not cross but are relatively parallel to one another. The curves of Figure 31 indicate that the pilot opinion when plotted against β_{DR} is more dependent upon ζ_{DR} than upon ϕ/β. The β_{DR} parameter was observed by the pilots and influenced their opinions of the lateral flying qualities.

CONCLUSIONS

Although the lack of abundance of data collected and the inherent control system deficiencies in this investigation render the results to be somewhat qualitative, it is concluded that:

1. The K_3/K_1 parameter influences pilot opinion of lateral flying qualities, especially when the dutch roll damping is adequate to suppress the more objectionable combined rolling and yawing oscillations.

2. The magnitude of the β oscillation is a parameter which influences pilot opinion of lateral flying qualities.

3. The greatest single factor which improves pilot opinion of lateral flying qualities is an increase in ζ_{DR}.

4. The minimum ζ_{DR} for a high performance fighter airplane is approximately 0.1.

5. Pilots prefer a minimum of aileron yaw.

6. When the "steady state" roll rate is permitted to vary with changes in $Cn_{\zeta a}$, pilot opinion favors the aileron adverse yaw over the proverse condition.

RECOMMENDATIONS

1. Because of the difficulty encountered in separating the deficiencies in the airplane's lateral responses from the deficiencies in the control system, it is strongly recommended that:

   a. The electric control stick be altered to provide a greater force gradient per inch of stick displacement.

   b. The break-out force and the stick center dead-zone be reduced.

   c. The autopilot system be examined with a view toward increasing the capability of achieving high feedback gains.

   d. Consideration be given to positioning the aileron servo potentiometers at the ailerons.

2. It is further recommended that investigation be continued into the parameters K_3/K_1 and β in the region of $\phi/\beta = 2$ to 5 and $\zeta_{DR} > .1$. Further flight study concentrated in this area should prove useful in fixing the values of K_3/K_1 and β as flying qualities criteria.

REFERENCES

1. Flying Qualities of Piloted Airplanes, U.S. Military Specification MIL-F-8785 (ASG), 1 September 1954 (Amendment 3, 12 November 1957).

2. Goodyear Aircraft Corporation: Operation and Maintenance of L3 GEDA. Akron, Ohio, 1 June 1953.

3. O'Hara, J.R. and Ebert, E.L.: A Preliminary Evaluation of the NAvion as a Lateral-Directional Flight Simulator for Use in the Investigation of Flying Qualities Criteria. Princeton University Aeronautical Engineering Report No. 509, 1960.

4. Wiltsie, R.E. and Link, S.T.: Flight Simulation of the Longitudinal Motions of Another Aircraft. Princeton University Aeronautical Engineering Report No. 508, 1960.

5. Perkins, Courtland D. and Hage, Robert E.: Airplane Performance Stability and Control. John Wiley and Sons, New York, 1949.

6. Gowen, Norman E.: Lateral Stability Investigation of an F-100 Airplane. WADC Technical Report 57-563, November 1957.

7. Northrop Aircraft, Inc.: Method of Analysis and Synthesis of Aircraft Flight Control Systems. BUAER Report AE-61-4-I, March 1952.

8. DeLong, George E. and Moore, Robert S.: The Determination of Lateral Stability Derivatives for a NAvion Airplane from Steady State Dynamic Flight Testing. Princeton University Aeronautical Engineering Report No. 388, May 1957.

9. Liddell, Charles R. et al: A flight Study of Requirements for Satisfactory Lateral Oscillatory Characteristics of Fighter Aircraft. NACA RM A-51E16.

10. Creer, Brent Y. et al: A Pilot Opinion Study of Lateral Control Requirements for Fighter-Type Aircraft. NASA MEMO 1-29-59A, March 1959.

11. Harper, Robert R.: In-Flight Simulation of Re-entry Vehicle Handling Qualities. IAS Paper 60-93.

12. Ashkenas, Irving L. and McRuer, Duane T.: The Determination of Lateral Handling Quality Requirements from Airframe-Human Pilot System Studies. WADC Technical Report 59-135.

13. Ashkenas, I.L. and McRuer, Duane T.: Flight Control-Airframe System Optimization. IAS Preprint No. 59-12, January 1959.

TABLE I

SPECIFICATIONS FOR THE NAVION AIRPLANE

I. Continental E-185 Power Plant

Maximum continuous power = 185 HP at 2300 rpm

Take-off power = 205 HP at 2600 rpm

Hertzell controllable pitch propeller

II. Fuselage

Length over-all	27.25 ft.
Maximum width	4.14 ft.
Maximum depth	4.40 ft.
Fineness ratio	6.2

III. Wing

Total area	184.34 $ft.^2$
Span	33.38 ft.
Aspect Ratio	6.05
Taper Ratio	0.54
Dihedral Angle	7.50 deg.
Root Chord	7.20 ft.
Mean Aerodynamic Chord	63.35 in.
Incidence Angle	
Root	2.0 deg.
Tip	- 1.0 deg.
Sweepback of Leading Edge	3.0 deg.
Twist	
Geometric	3.0 deg.

TABLE I (continued)

Airfoil Section	
Root	NACA 4415R
Tip	NACA 6410R
Flaps, 40 deg., Plain	
IV. Aileron	
Area	2.16 ft.^{2}
Span	61.99 inc.
Deflection	30 deg. up; 20 deg. dwn.
Control	Wheel Throw
Aerodynamic Balance	Frise-type nose
Static Balance	Streamlined Weight
Trim Tab	Fixed Bend Tab
Ratio of Aileron Chord to Wing Chord	0.284
V. Horizontal Tail	
Total Area	43.05 ft.^{2}
Span	13.17 ft.
Aspect Ratio	4.02
MAC	3.34 ft.
Airfoil Sections, Root & Tip	NACA 0012
Incidence Angle	- 3.0 deg.
VI. Elevator	
Total Area	14.10 ft.^{2}
Span	73.58 in.
Deflection	30 deg. up; 20 deg. dwn.
Deflection Trim Tabs (32 in. span, 4-1/2 in. Chord)	$\pm$ 30 deg.
Root Chord	1.5 ft.
Tip Chord	1.0 ft.

TABLE I (continued)

VII. Vertical Tail	
Area	12.93 ft.^{2}
Span	4.05 ft.
Airfoil Section	
Root	NACA 0013.2 Modified
Tip	NACA 0012-64 Modified
Incidence Angle	2 deg. nose left
VIII. Rudder	
Area	6.05 ft.^{2}
Deflection	17 deg. L.; 23 deg. R.
Trim Tab	Fixed bend tab
Rig	3 deg. Right
IX. Miscellaneous	
Weight	
Basic	2129 lbs.
Fuel (40 gal.)	240 lbs.
Pilots (2 with parachutes)	410 lbs.
Gross weight	2779 lbs.
Center of Gravity Position	29.5 MAC
Tail Length	16.88 ft.

TABLE II

LATERAL EQUATION DERIVATIVES FOR POINTS

EXAMINED ON THE $\frac{\phi}{\beta}$ ζ PLANE

POINTS EXAMINED BY ANALOG MEANS ONLY

POINT	C_L	Cy_β	$C\ell_r$	$C\ell_p$	μ	Jx	Jz	Cn_r	$C\ell_\beta$	Cn_p	Cn_β
I	.1	-.8	+.04	-.4	70	.025	.2	-0.6	-0.18	-.01	+0.11
II								-1.4	-0.18		+0.10
III								-0.6	-0.13		+0.13
IV								-1.8	-0.12		+0.13
V								-0.6	-0.06		+0.18
VI								-1.8	-0.05		+0.18
VII								-0.5	-0.02		+0.20
VIII								-1.8	-0.02		+0.18
IX								-0.5	-0.01		+0.20
X								-1.8	-0.01		+0.20

POINTS EXAMINED BY ANALOG AND FLIGHT EVALUATION

III_F	0.5							-0.6	-0.13		+0.13
IV_F								-1.8	-0.12		+0.13
V_F								-0.6	-0.06		+0.18
VI_F								-1.8	-0.05		+0.18

TABLE III

IDENTIFICATION OF EVALUATION POINTS ON

THE $\frac{\phi}{\beta}$ ζ PLANE

POINTS EXAMINED BY ANALOG MEANS ONLY

POINT	ϕ/β	ζ_{DR}
I	8.10	0.112
II	9.52	0.267
III	5.30	0.116
IV	5.62	0.328
V	1.90	0.11
VI	2.00	0.31
VII	0.607	0.096
VIII	0.711	0.3
IX	0.299	0.097
X	0.316	0.288

POINTS EXAMINED BY ANALOG AND FLIGHT EVALUATION

III_F	5.30	0.06
IV_F	5.62	0.13
V_F	1.90	0.06
VI_F	2.00	0.13

TABLE IV

NUMERICAL VALUES FOR BASIC NAVION

STABILITY DERIVATIVES

NONDIMENSIONAL DERIVATIVES	VALUE	DIMENSIONAL DERIVATIVE	VALUE
Cy_β	-0.592	Yv	-0.216
$C\ell_r$	+0.117	Lr	+1.95
$C\ell_\beta$	-0.0554	Lβ	-9.76
$C\ell_p$	-0.441	Lp	-7.40
Cn_r	-0.0932	Nr	-0.461
$Cn_{\xi a}$	-0.0034	Nδa	-0.178
Cn_β	+0.0918	Nβ	+4.81
Cn_p	-0.0758	Np	-0.376
$Cy_{\delta r}$	+0.158	Yδr	+0.057
$C\ell_{\xi a}$	+0.115	Lξa	+20.50
$C\ell_{\delta r}$	+0.0116	Lδr	+2.05
$Cn_{\delta r}$	-0.0691	Nδr	-3.62

The nondimensional derivatives were dimensionalized using the following values:

h = 6500 ft. SDA $\qquad$ U_o = 120 MPH TAS

τ = 1.37 sec $\qquad$ μ = 7.24

J_X = 0.0218 $\qquad$ J_Z = 0.0735

TABLE V

DEFINING EQUATIONS FOR EQUIVALENT
AND
ARTIFICIAL STABILITY DERIVATIVES

$L\beta'' = L_\beta + K_4 L_{\delta a} + K_8 L_{\delta a}$

$Lr'' = L_r + K_6 L_{\delta r} + K_{10} L_{\delta a}$

$Lp'' = L_p + K_5 L_{\delta r} + K_9 L_{\delta a}$

$L\delta a'' = K_{13} L_{\delta a} + K_7 L_{\delta r}$

$L\delta r'' = K_{14} L_{\delta r}$

$N\beta'' = N_\beta + K_4 N_{\delta r} + K_8 N_{\delta a}$

$Nr'' = N_r + K_6 N_{\delta r} + K_{10} N_{\delta a}$

$Np'' = N_p + K_5 N_{\delta r} + K_9 N_{\delta a}$

$N\delta a'' = K_{13} N_{\delta a} + K_7 N_{\delta r}$

$N\delta r'' = K_{14} N_{\delta r}$

$Yv'' = Y_v + K_4 Y_{\delta r}$

$Yp'' = K_5 Y_{\delta r}$

$Y\delta r'' = K_{14} Y_{\delta r}$

$L\phi'' = K_{11} L_{\delta a}$

$N\phi'' = K_{11} N_{\delta a}$

K_4 = deg rudder/deg β

K_5 = deg rudder/deg/sec $\dot{\phi}$

K_6 = deg rudder/deg/sec $\dot{\psi}$

K_7 = deg rudder/inch stick

K_8 = deg aileron/deg β

K_9 = deg aileron/deg/sec $\dot{\phi}$

K_{10} = deg aileron/deg/sec $\dot{\psi}$

K_{11} = deg aileron/deg ϕ

K_{13} = deg aileron/inch stick

TABLE VI

SOLUTIONS OF THE SIMULTANEOUS EQUATIONS

FOR FEEDBACK GAIN CONSTANTS

$K_4 = 1.312 - .002415\ L\beta'' - 0.2774\ N\beta''$

$K_5 = -0.125 - .002415\ Lp'' - 0.2775\ Np''$

$K_6 = -0.174 - .002415\ Lr'' - 0.2775\ Nr''$

$K_8 = 0.346 + 0.0490\ L\beta'' + 0.0278\ N\beta''$

$K_9 = 0.373 + 0.0490\ Lp'' + 0.0278\ Np''$

$K_{10} = 0.0828 + 0.0490\ Lr'' + 0.0278\ Nr''$

$$\frac{K_7}{K_{13}} = -\frac{20.5\ \frac{N_a''}{L_a''} + 0.178}{2.05\ \frac{N_a''}{L_a''} + 3.62} = \tau_{r_s}$$

TABLE VII

PILOT EXPERIENCE

Pilot	Organization	Flight Hours	Jet Hours	Years Flying
1	USN	2600*	400	12
2	USN	1750	0	7
3	USN	1250	500	6
4	Civilian	800**	0	15

(*) Graduate of USN Test Pilot School

(**) 150 of 800 hours is in glider aircraft

TABLE VIII

PILOT OPINION SCALE

Adjective Rating	Numerical Rating		Description
Good	1		Excellent, optimum
	2		Rapid response, comfortable to fly
	3		Mildly unpleasant characteristics
Satisfactory (Acceptable)	4		Acceptable for one flight condition, but Good for another
	5		Acceptable with unpleasant characteristics
	6		Difficult to track or to fly hands-off
Unsatisfactory (Unacceptable)	7		Weakly damped oscillations of moderate magnitude
	8		Unacceptable but flyable, requires constant pilot control
	9		Undamped oscillations tending toward divergence
Unflyable	10		Uncontrolable, divergent oscillations

Flight Conditions Investigated

1. Turns with bank angles between 10 and 30 degrees.

2. Abrupt turns with bank angles between 30 and 45 degrees.

FIGURE 1 (top) TEST AIRPLANE

FIGURE 2 (bottom) VANE BOOM

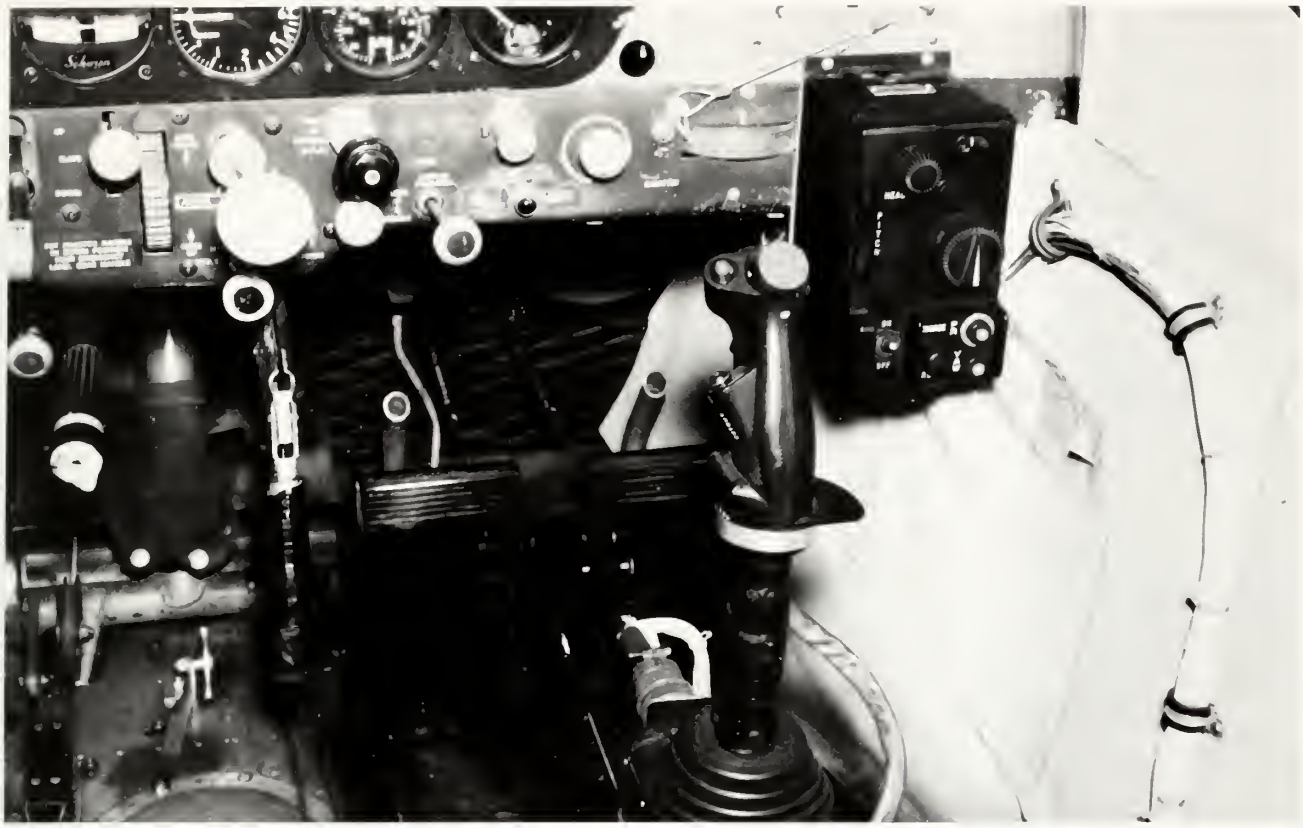

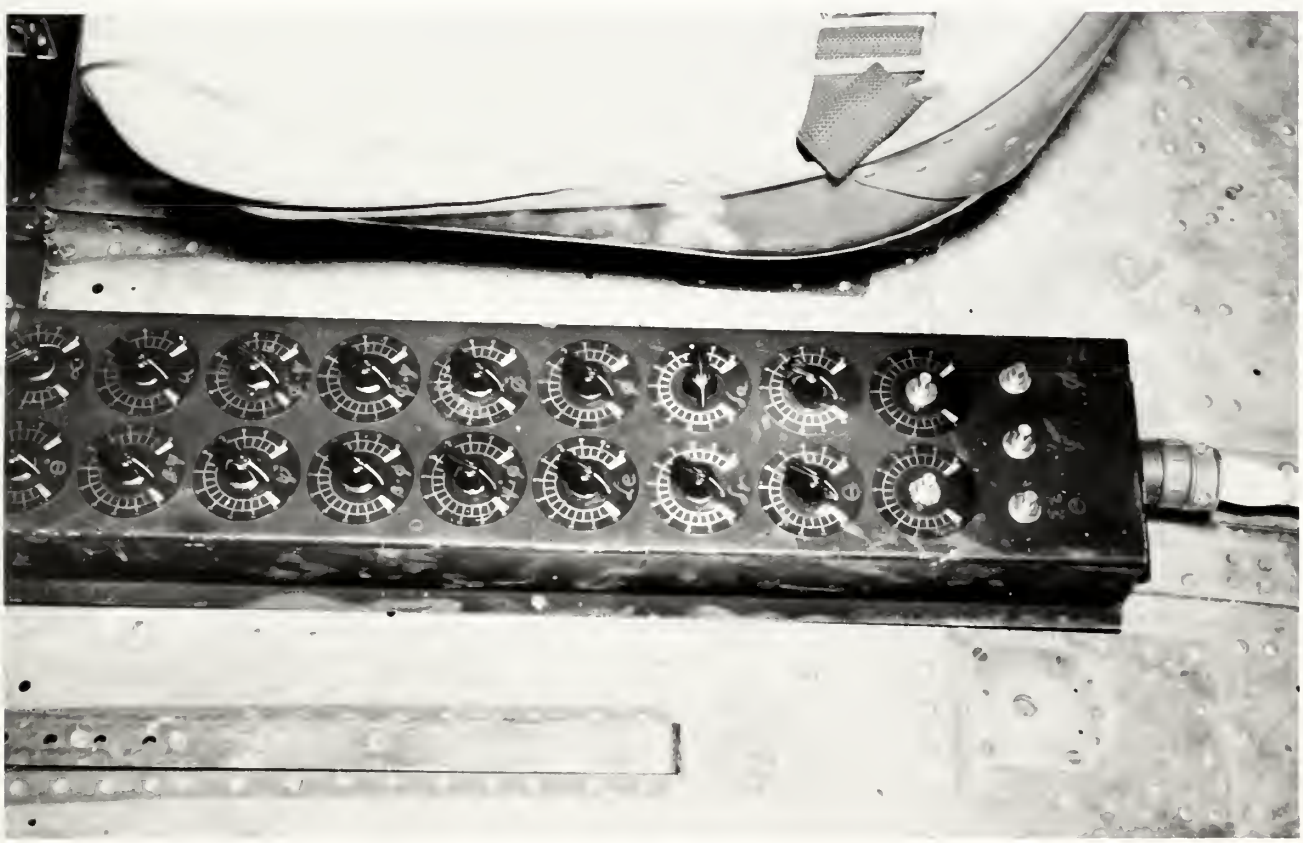

FIGURE 3 (top) COCKPIT CONFIGURATION

FIGURE 4 (bottom) GAIN POTENTIOMETER PANEL

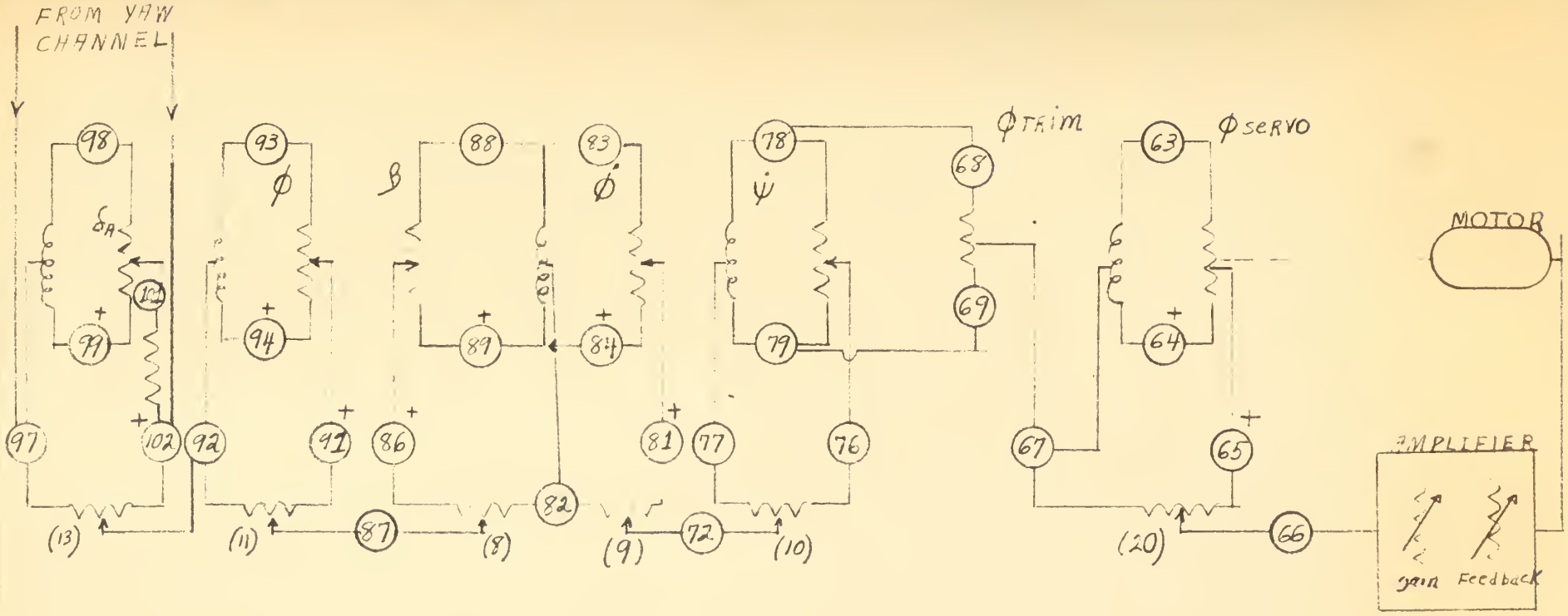

FIGURE 9

AUTOPILOT ROLL CHANNEL SUMMING CIRCUIT

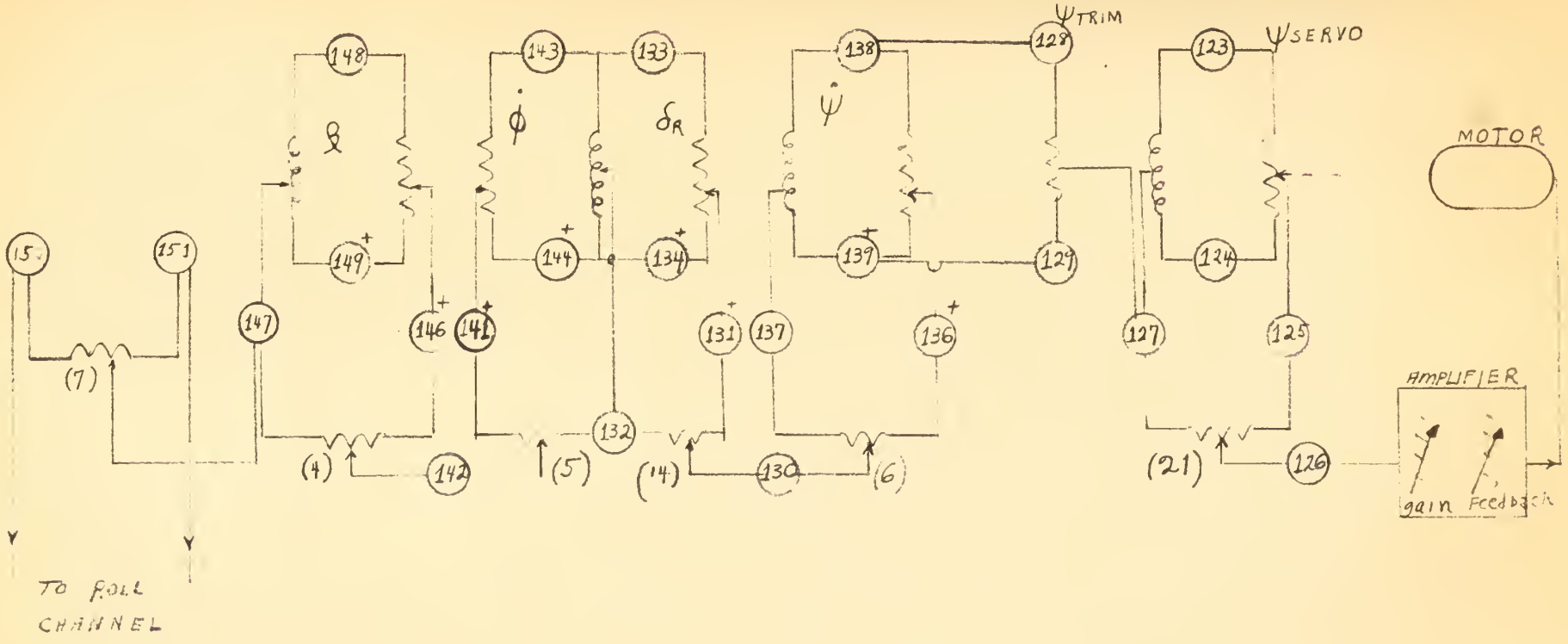

FIGURE

AUTOPILOT YAW CHANNEL SUMMING CIRCUIT

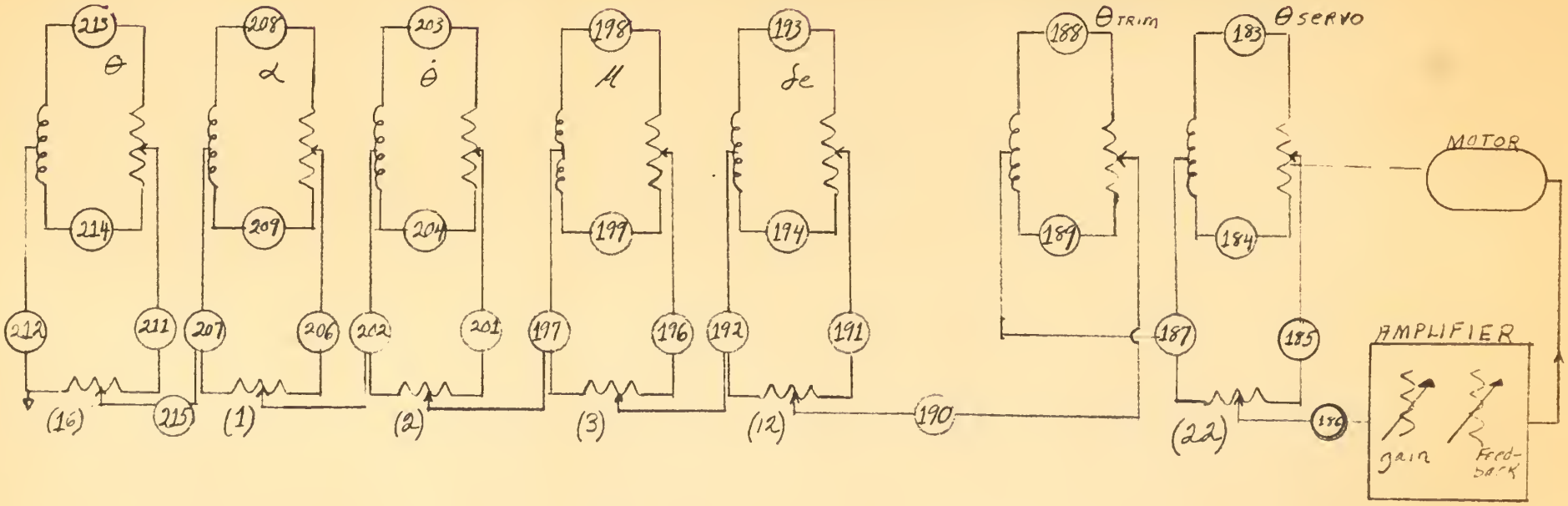

FIGURE 7

AUTOPILOT PITCH CHANNEL SUMMING CIRCUIT

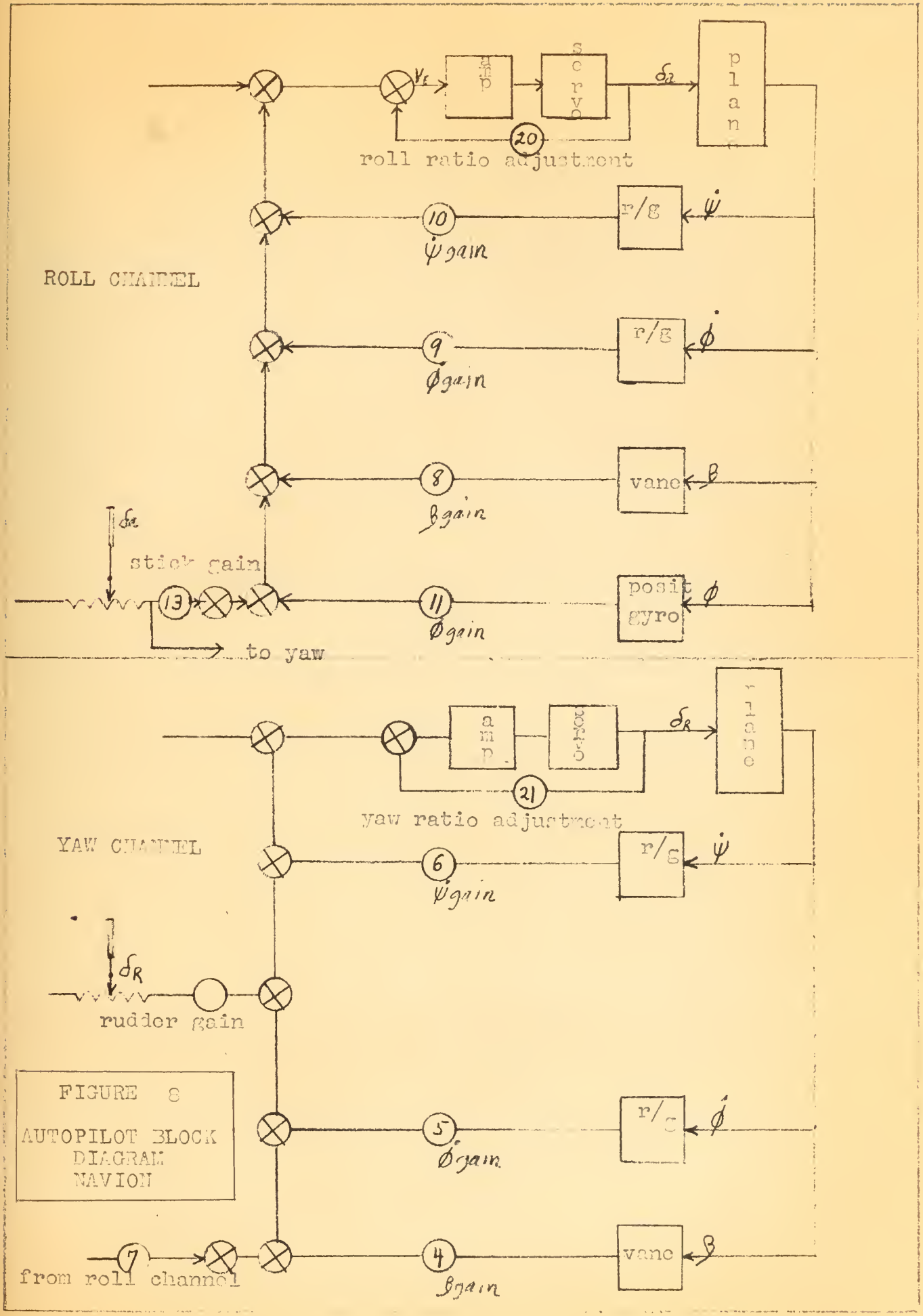

FIGURE 8

AUTOPILOT BLOCK DIAGRAM NAVION

FIGURE 9

AIRCRAFT CONTROL SYSTEM

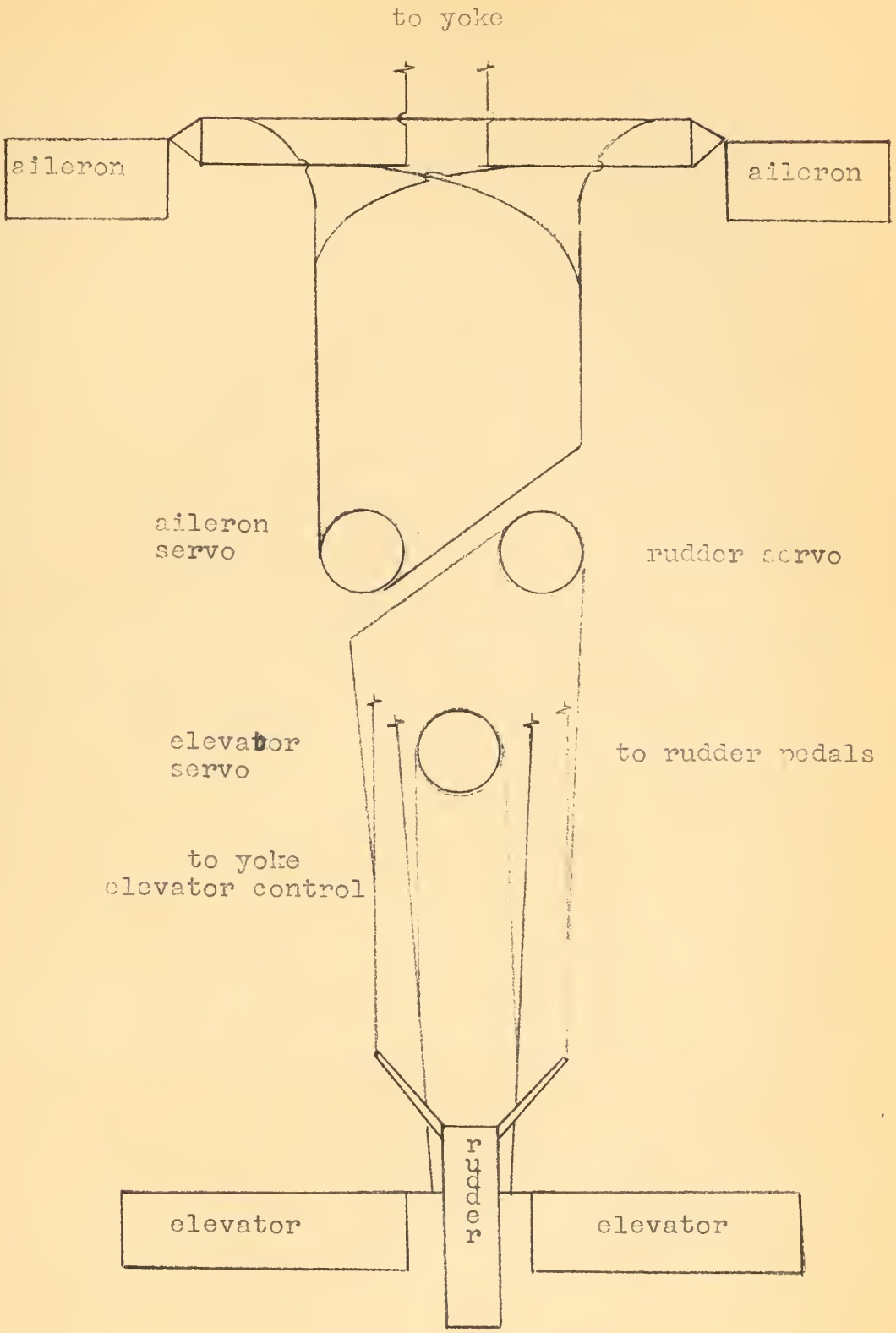

FIGURE 10

LATERAL CHARACTERISTIC EQUATION
ROOT LOCUS WITH VARYING C_{l_β}

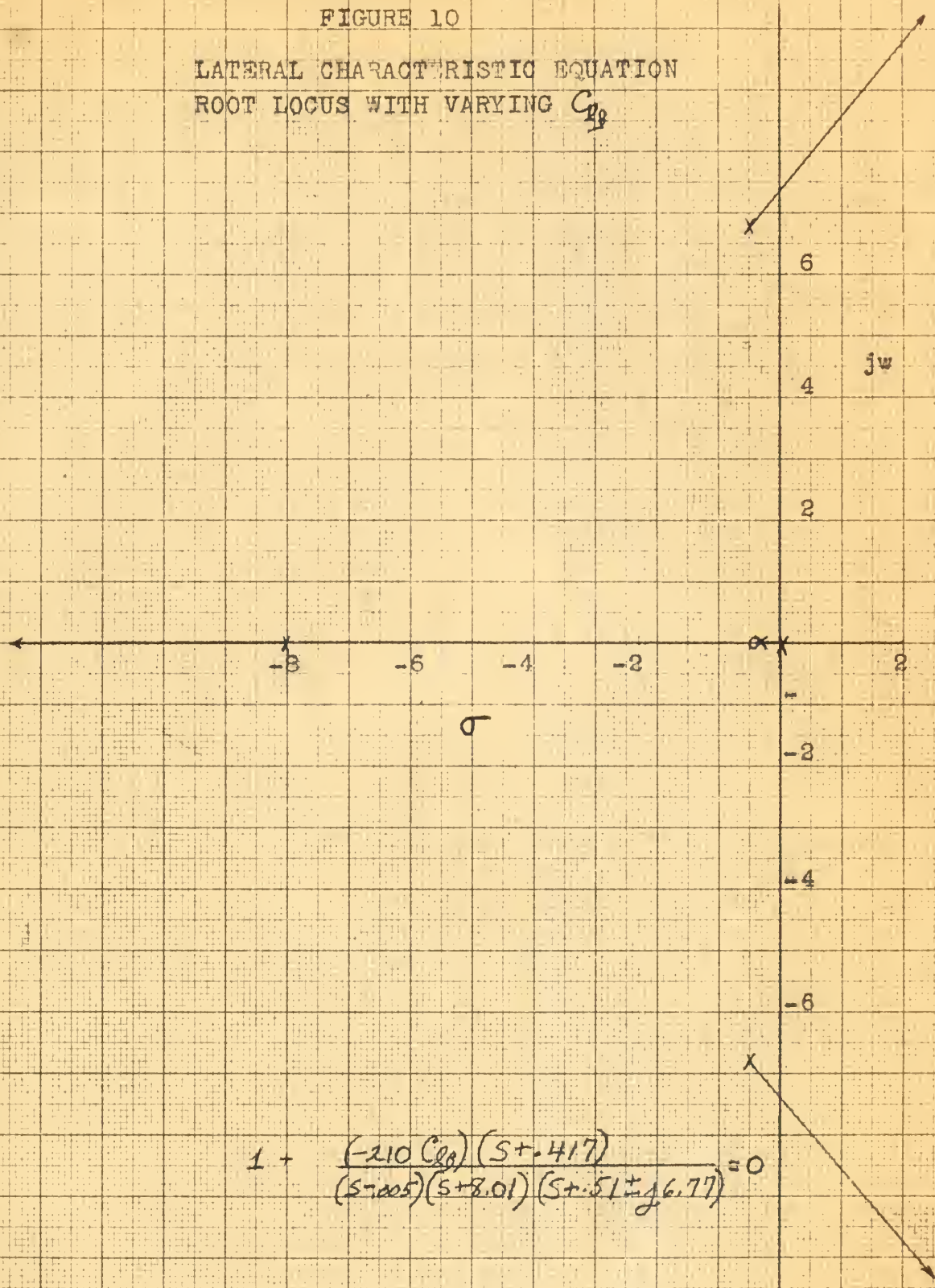

$$1 + \frac{(-210\,C_{l_\beta})(S+.417)}{(S+.005)(S+8.01)(S+.51 \pm j6.77)} = 0$$

FIGURE 11

LATERAL CHARACTERISTIC EQUATION
ROOT LOCUS WITH VARYING C_{n_r}

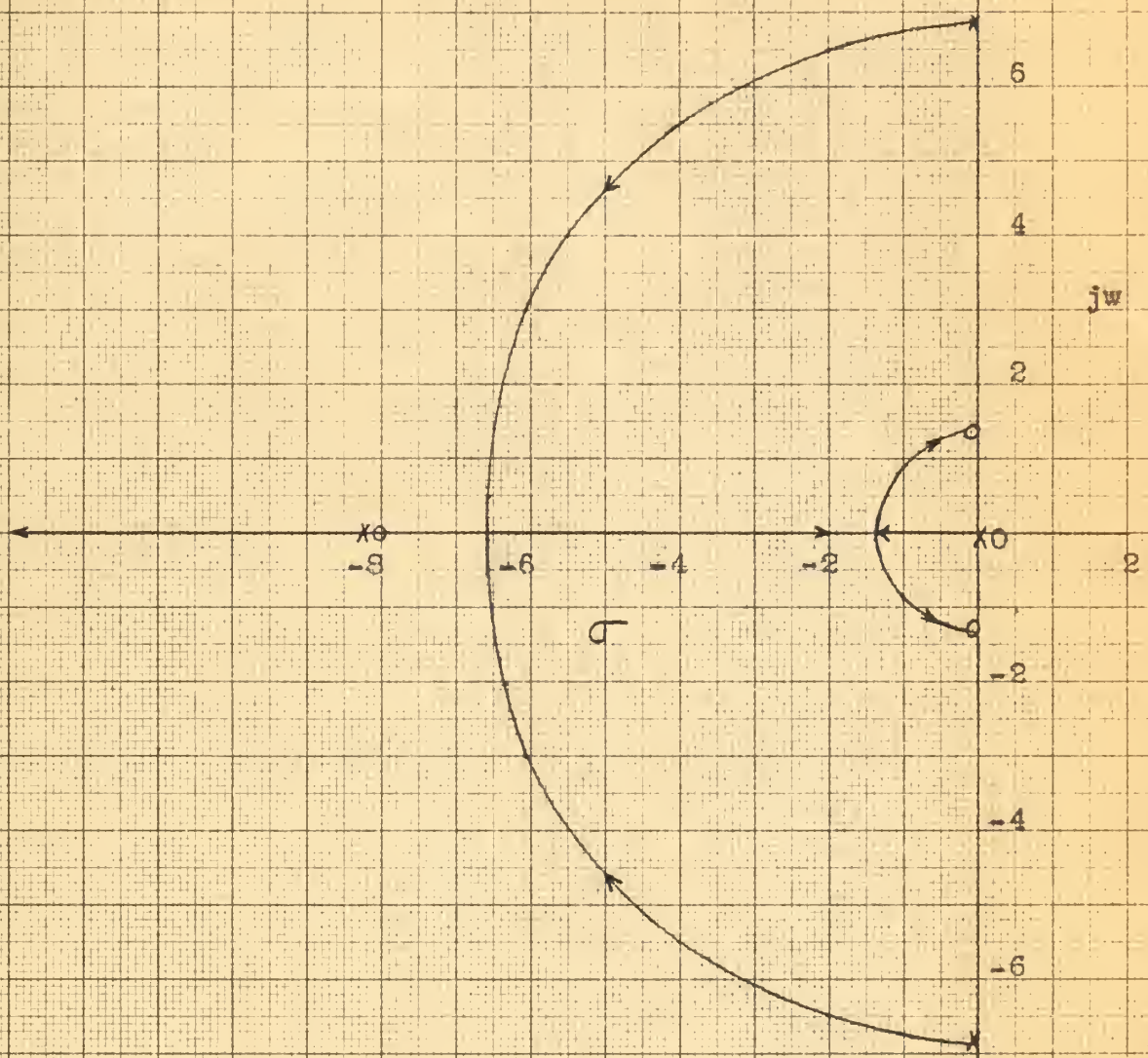

$$1 + \frac{(-2.5C_{n_r})(s+8.02)(s+.09 \pm j1.33)}{(s-.0148)(s+8.23)(s+.082 \pm j6.88)} = 0$$

FIGURE 12

LATERAL CHARACTERISTIC EQUATION
ROOT LOCUS WITH VARYING C_{n_β}

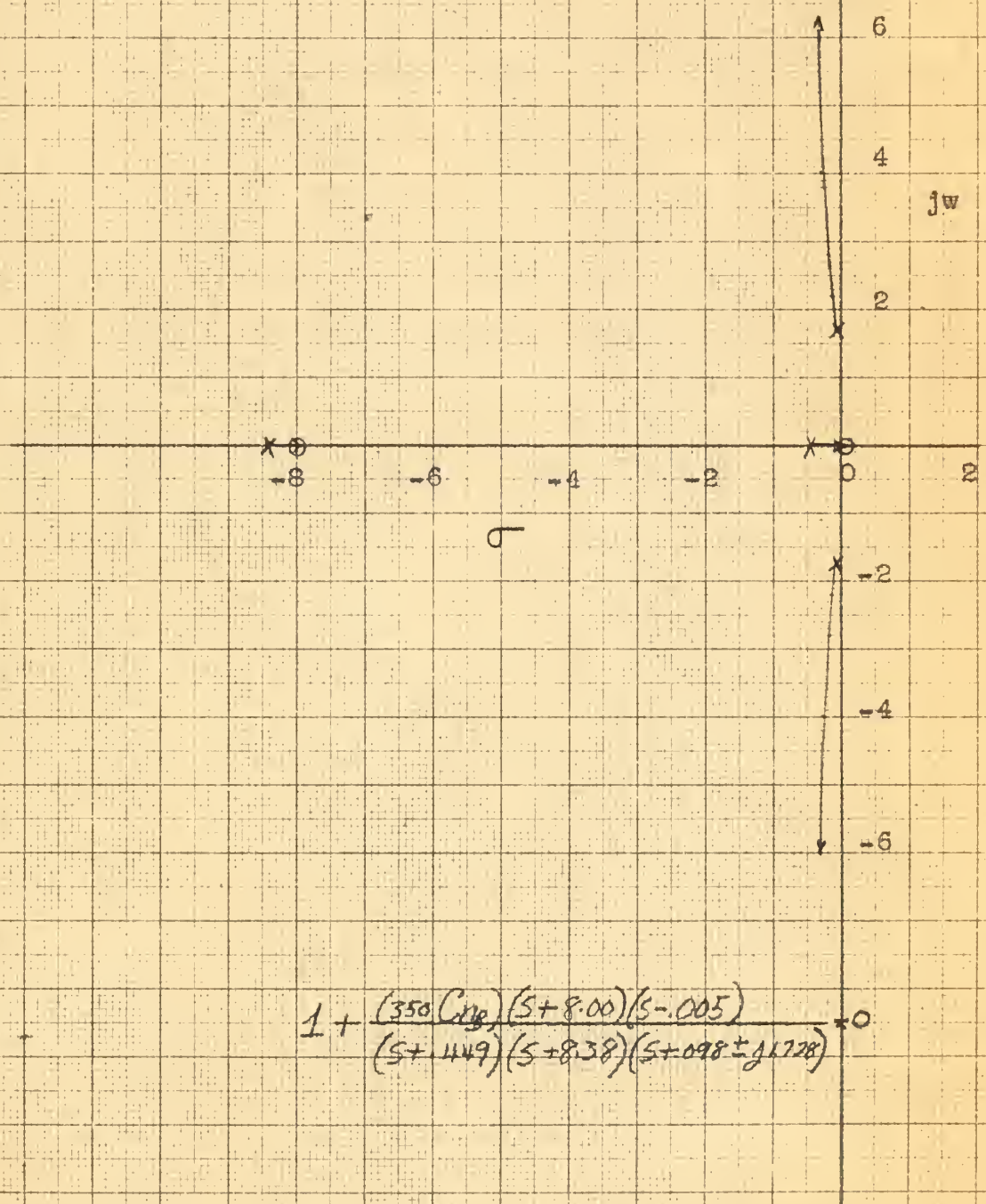

$$1 + \frac{(350 C_{n_\beta})(S+8.00)(S-.005)}{(S+.449)(S+8.38)(S+.098 \pm j1.728)} = 0$$

FIGURE 13

LATERAL CHARACTERISTIC EQUATION
ROOT LOCUS WITH VARYING C_{n_p}

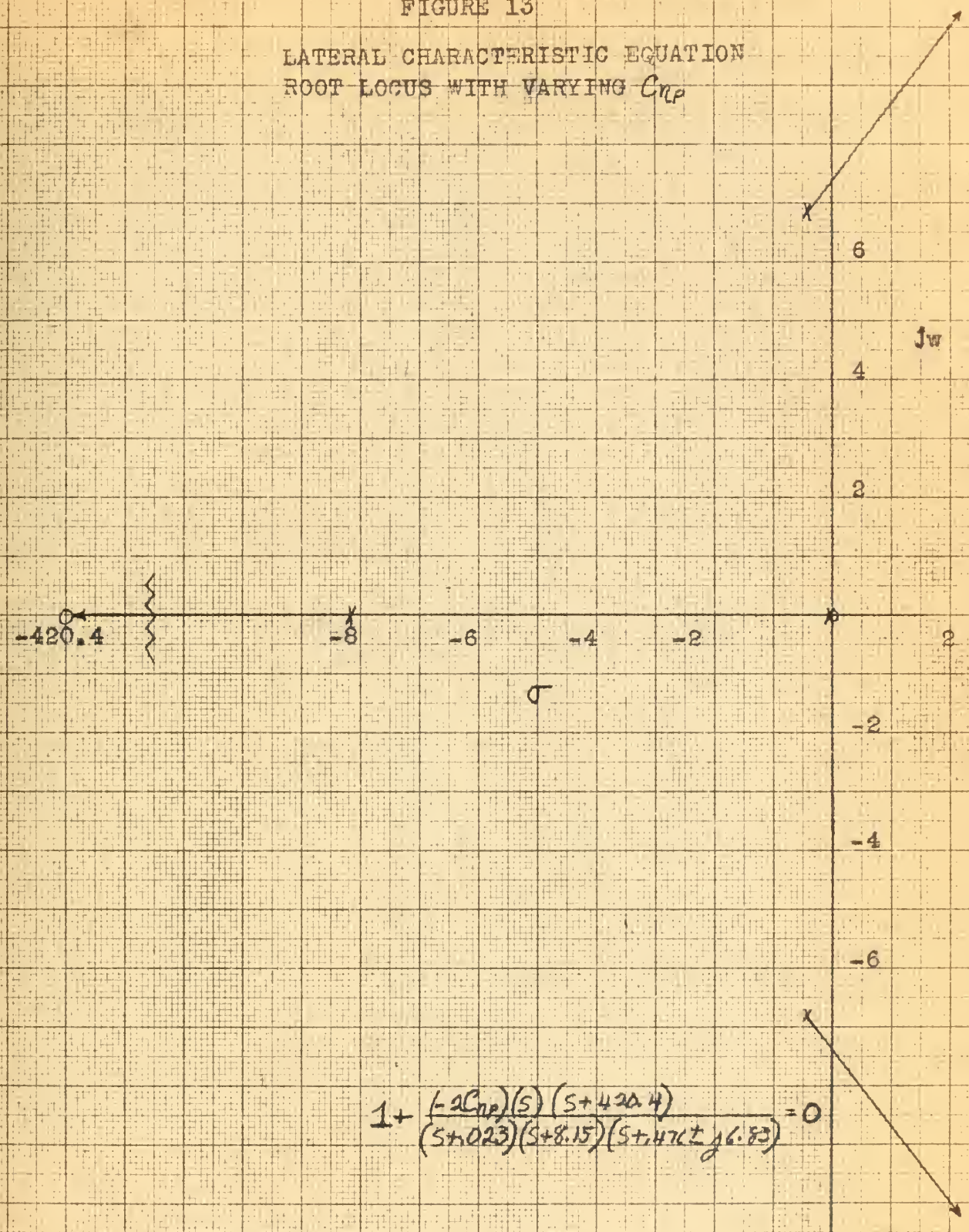

$$1+\frac{(-2C_{n_p})(S)(S+420.4)}{(S+.023)(S+8.15)(S+.47\pm j6.83)}=0$$

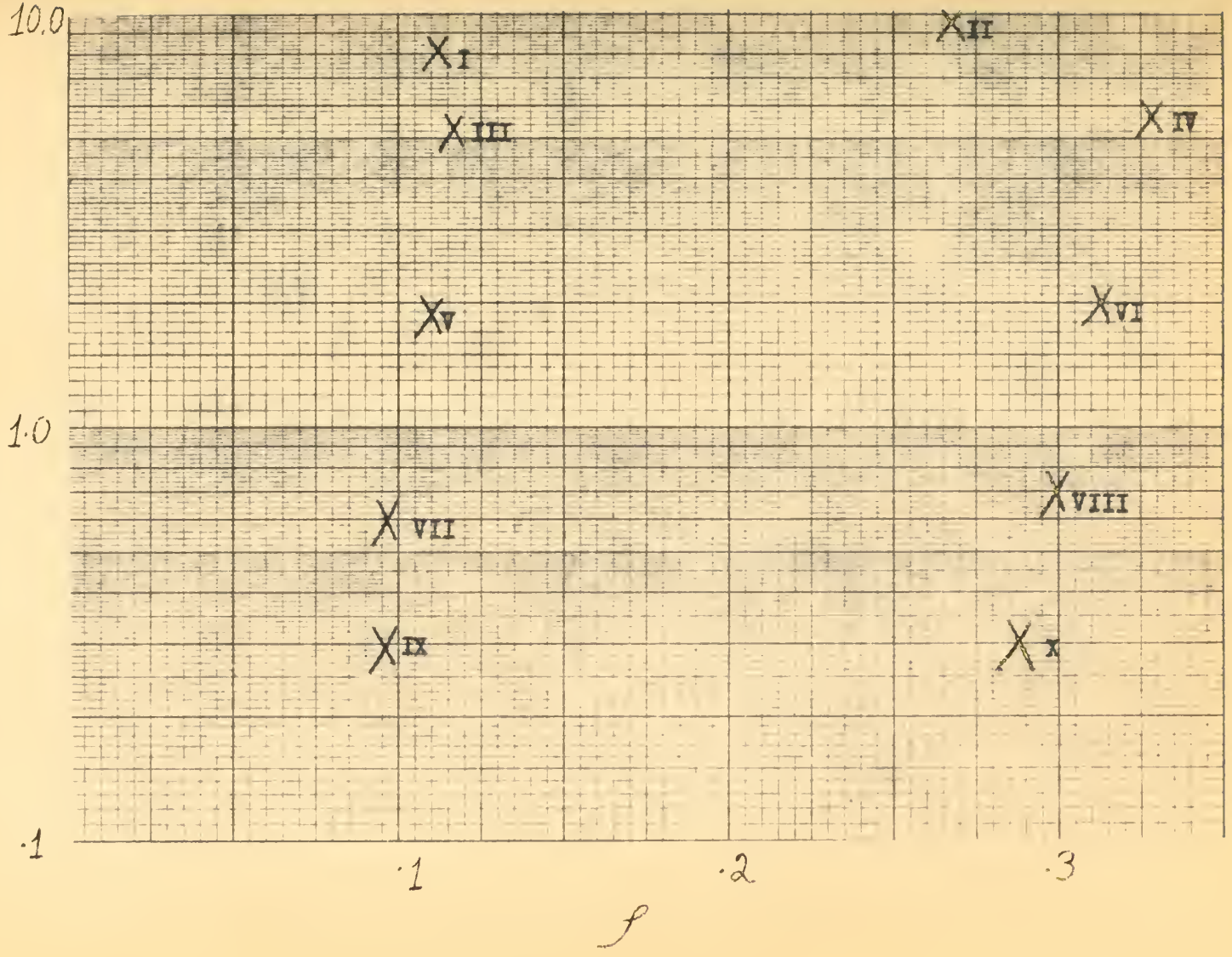
10.0
1.0
·1
·1
·2
·3
$\frac{\phi}{\varepsilon}$
f
XI
XII
XIII
XIV
XV
XVI
XVII
XVIII
XIX
X

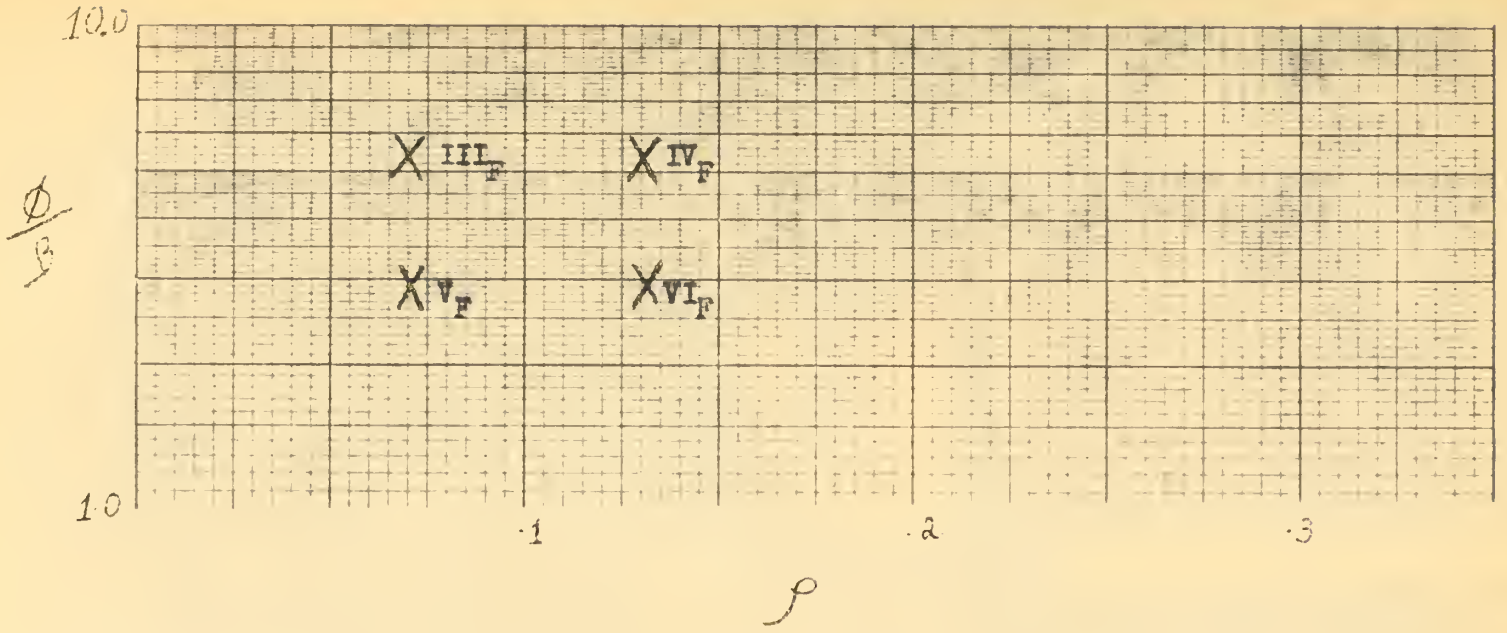

$\frac{\phi}{\beta}$ vs. ρ

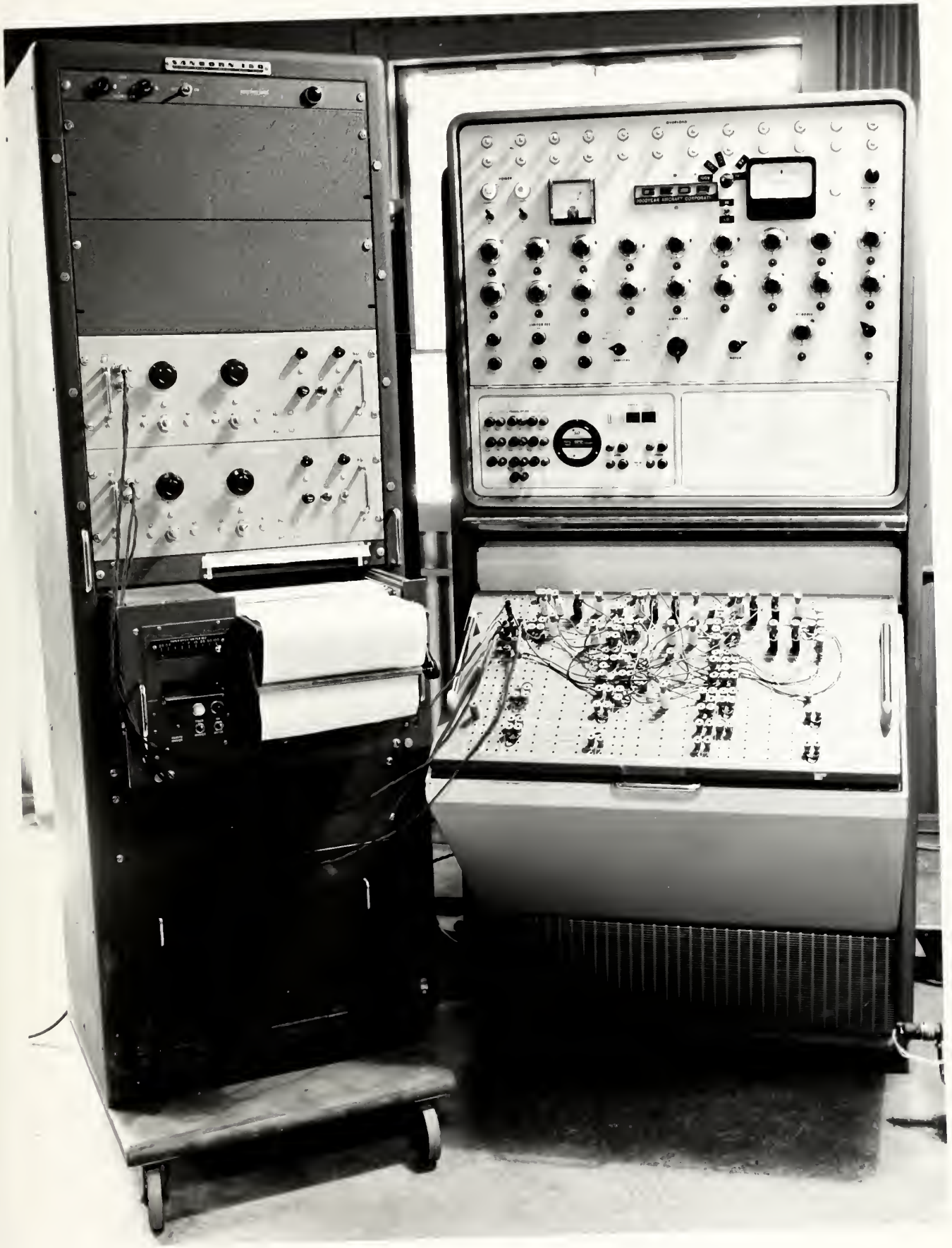

FIGURE 16

ANALOG COMPUTER AND RECORDER

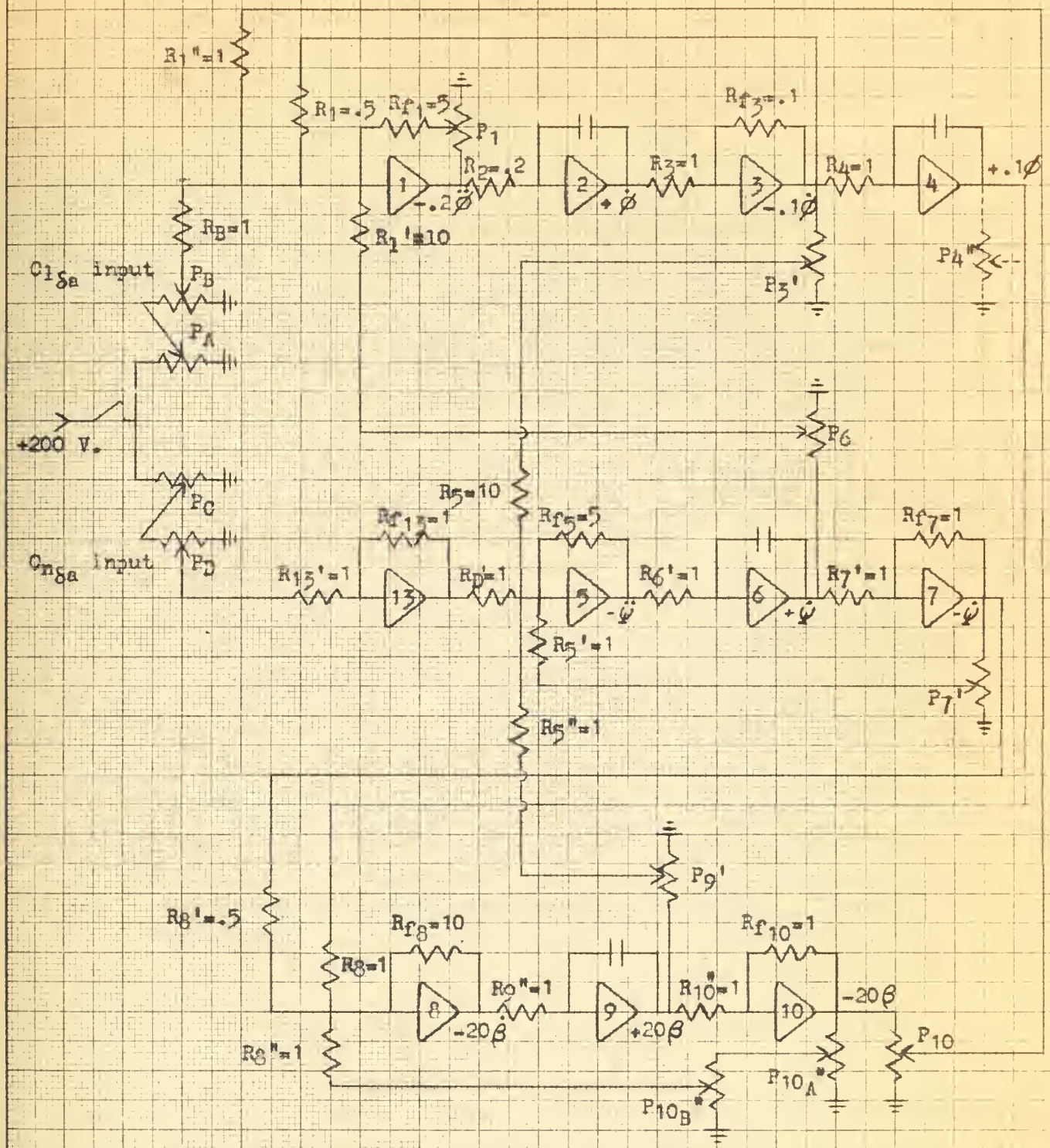

FIGURE 17

ANALOG COMPUTER DIAGRAM

Lateral-directional responses of a high performance airplane

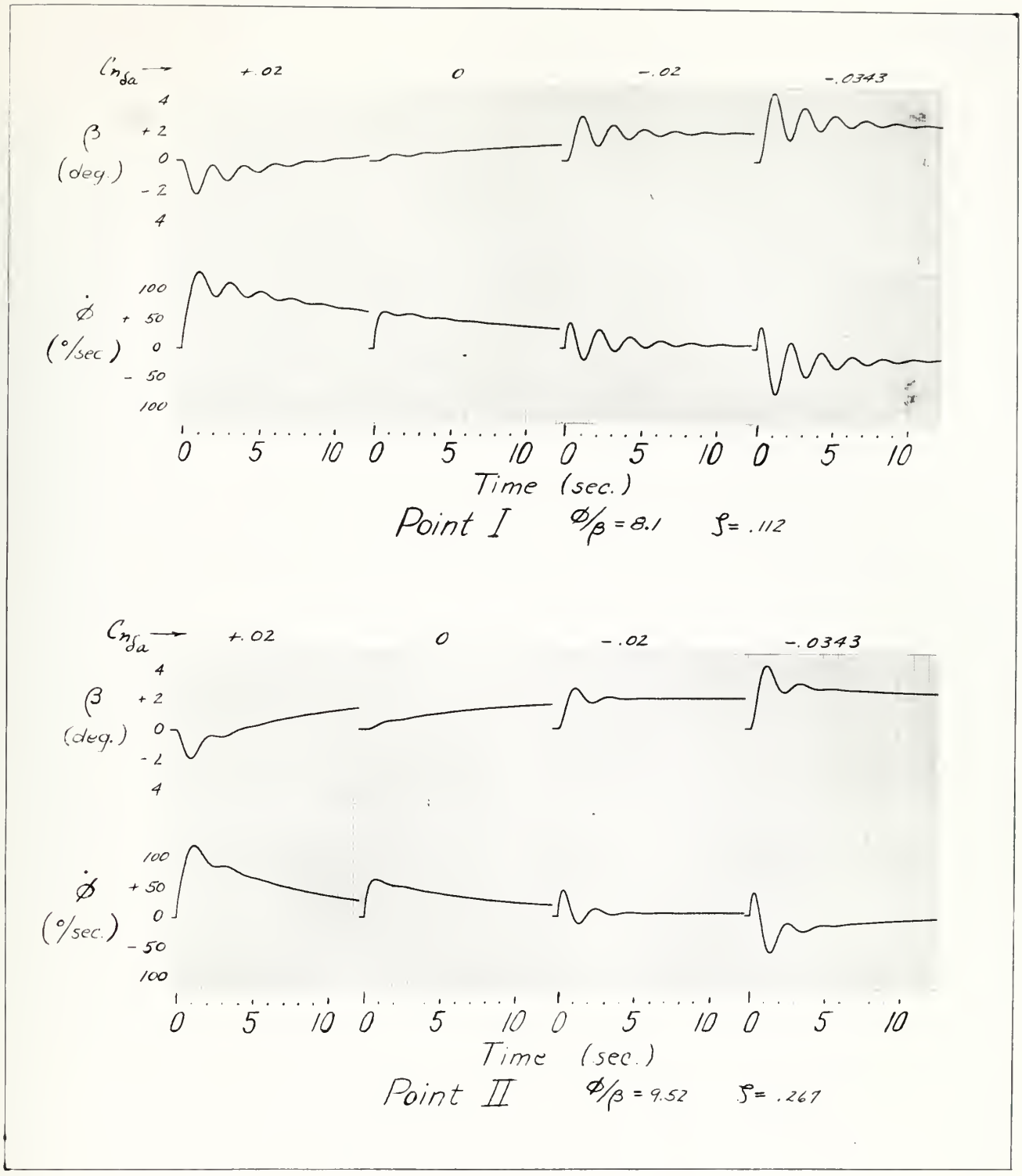

FIGURE 18

ANALOG RESPONSE TO 10° AILERON STEP INPUT
Theoretical Study

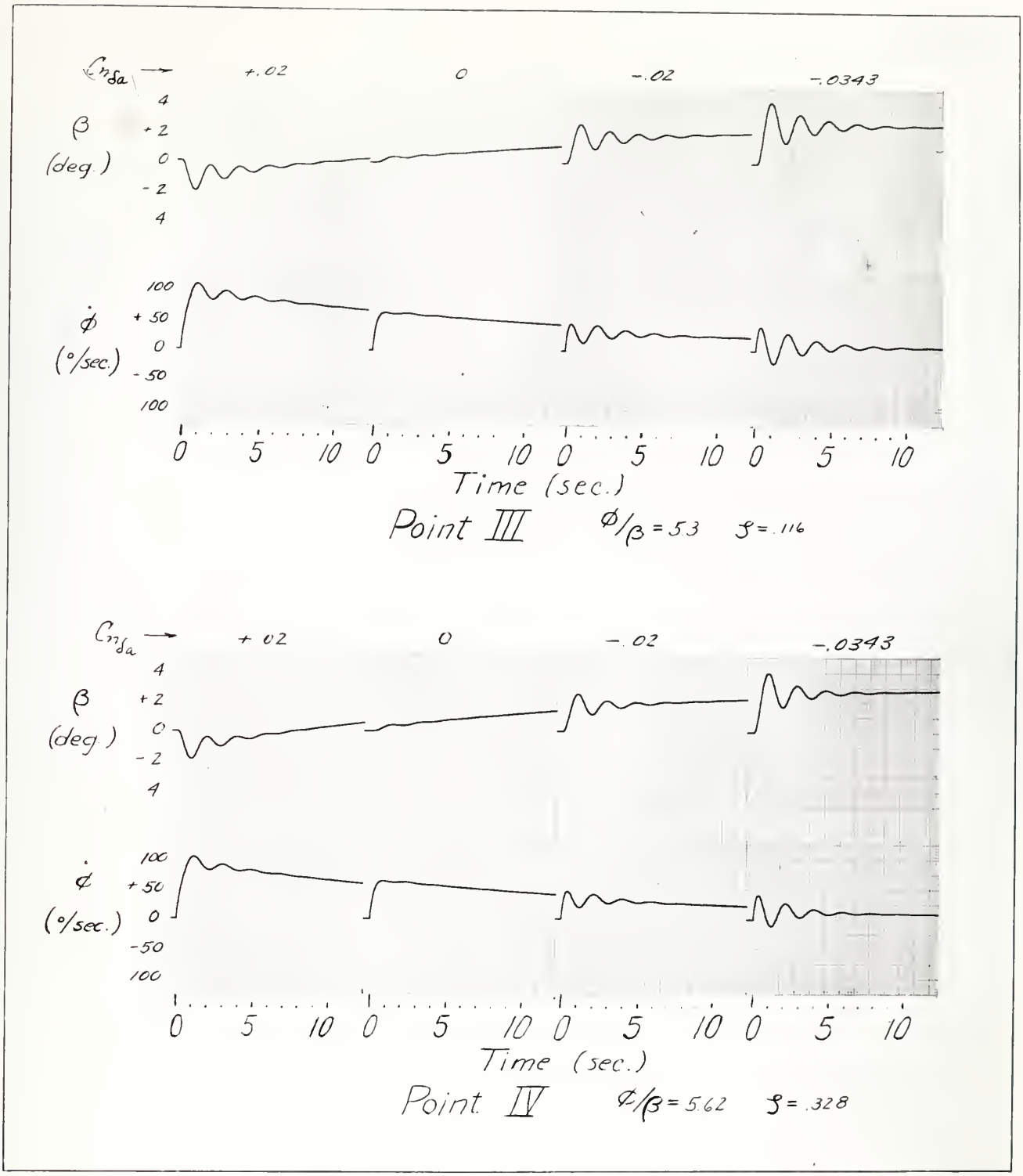

FIGURE 18

ANALOG RESPONSE TO 10° AILERON STEP INPUT
Theoretical Study

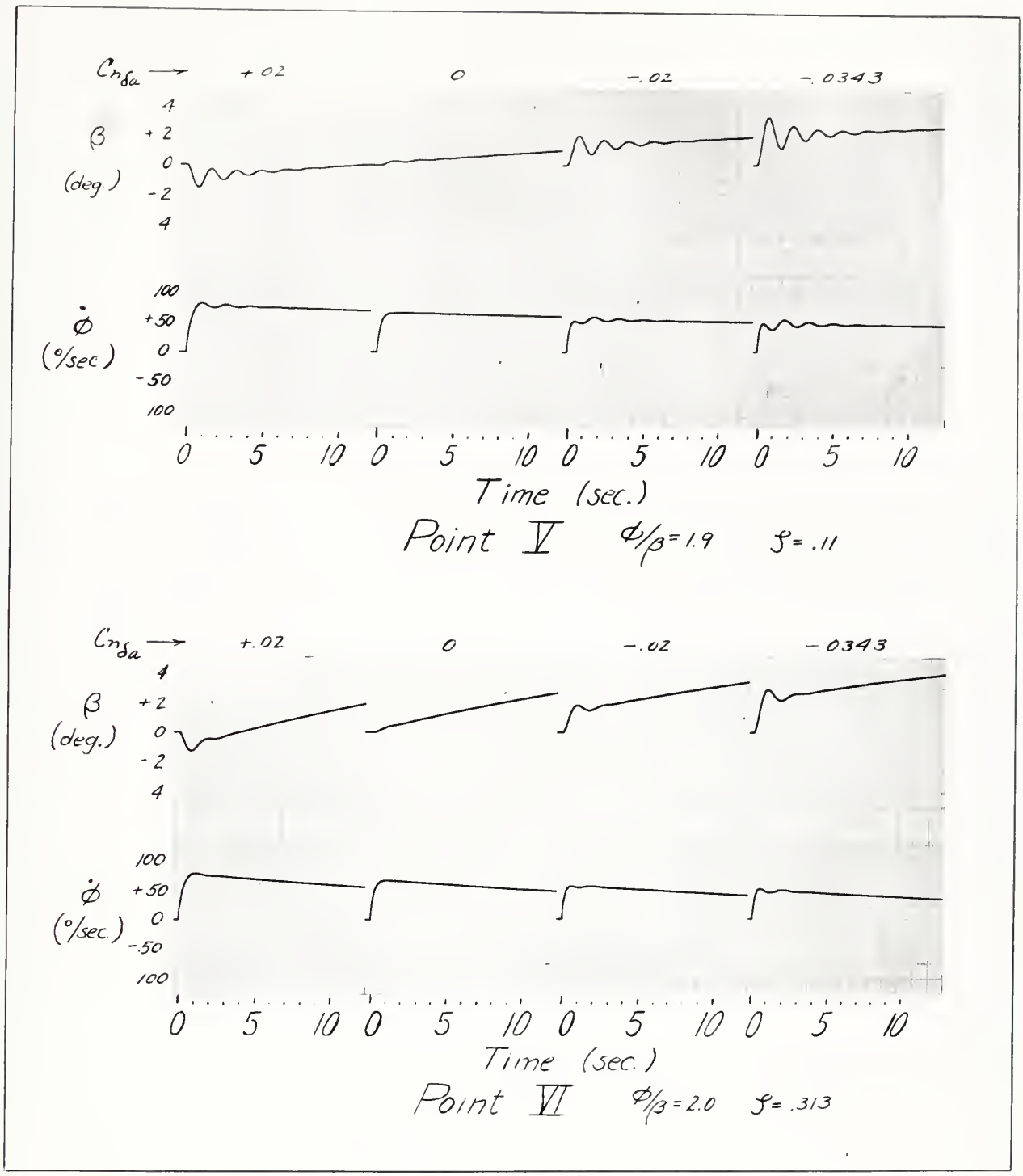

FIGURE 18

ANALOG RESPONSE TO 10° AILERON STEP INPUT
Theoretical Study

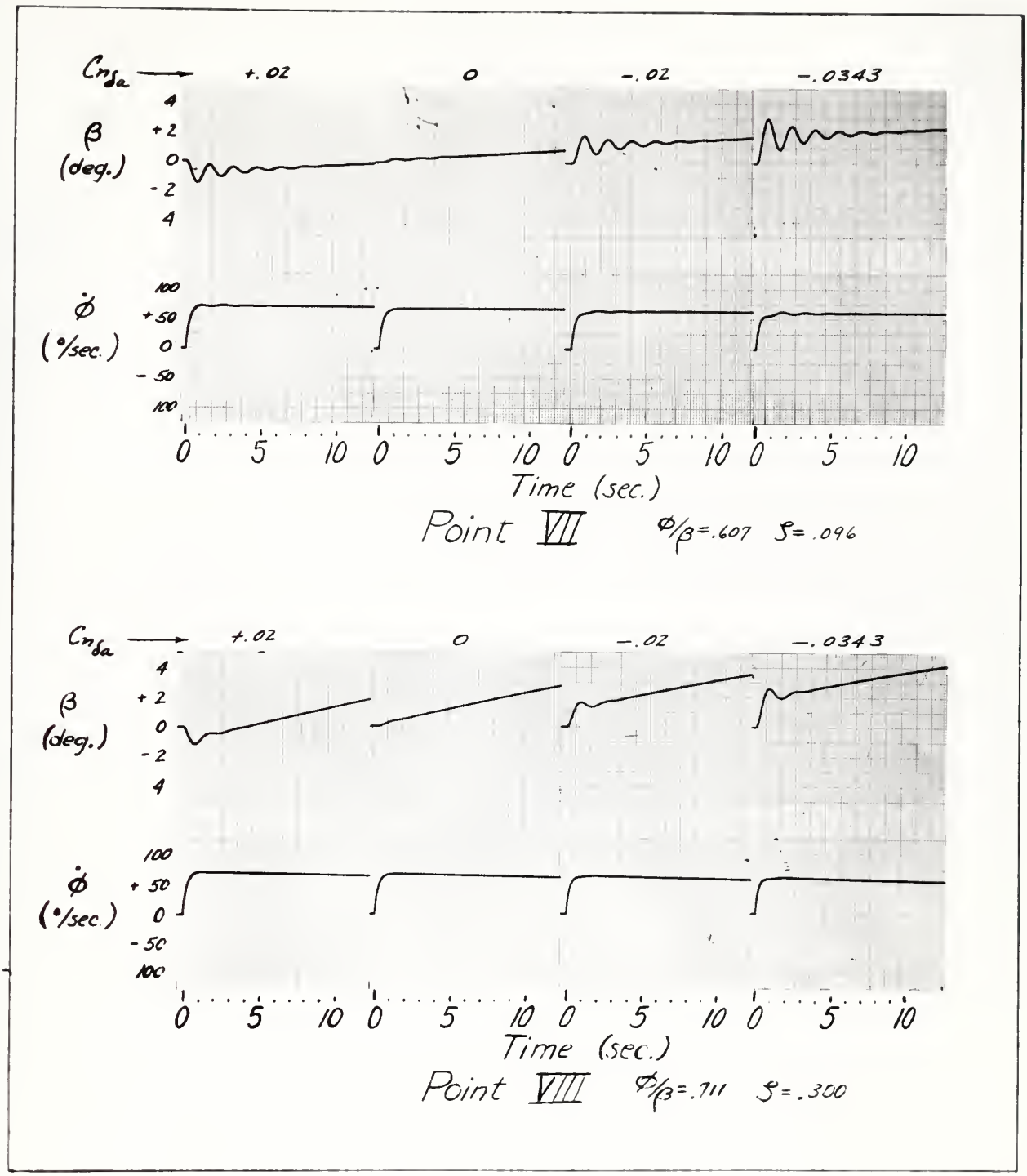

FIGURE 18

ANALOG RESPONSE TO 10° AILERON STEP INPUT
Theoretical Study

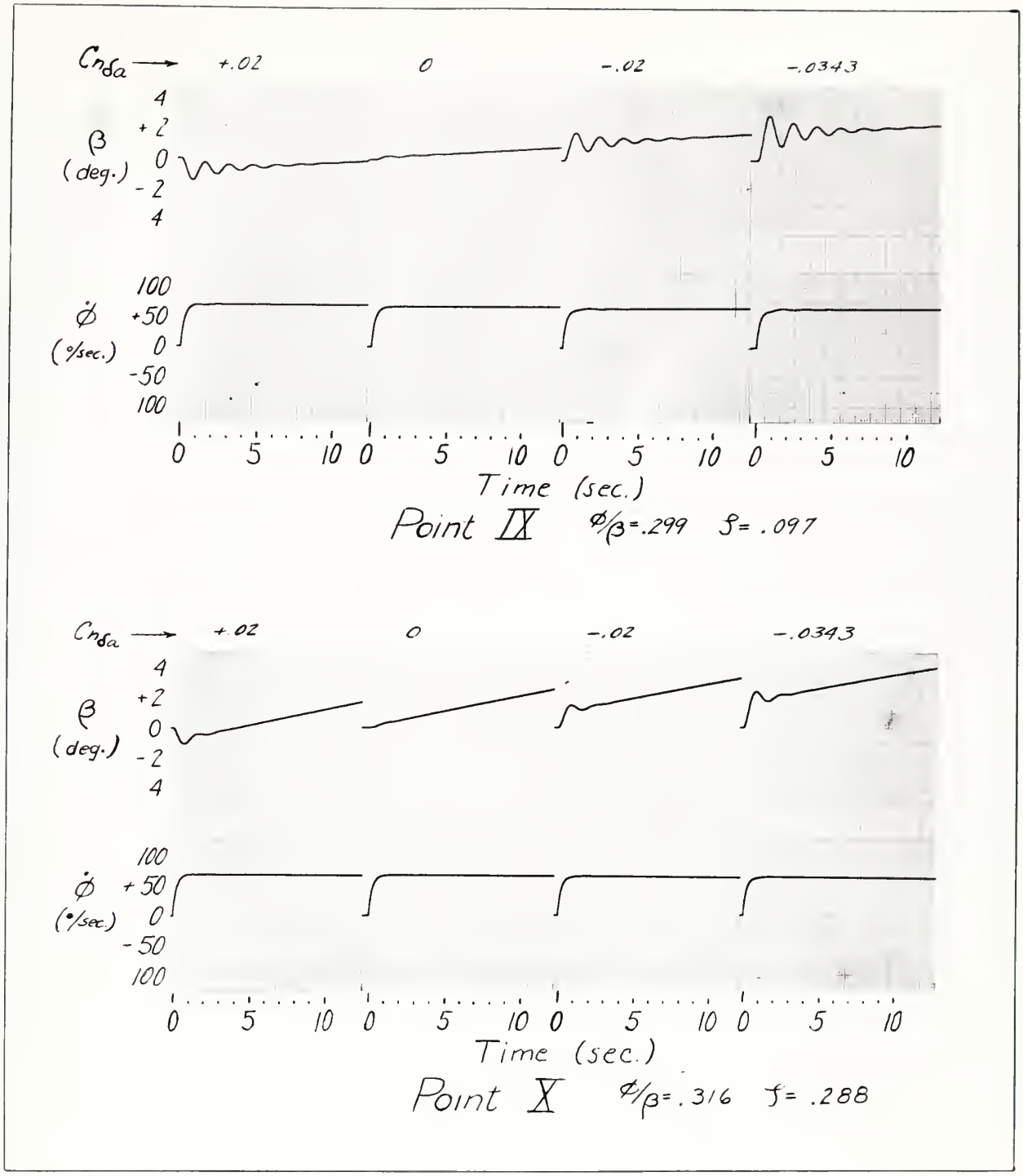

FIGURE 18

ANALOG RESPONSE TO 10° AILERON STEP INPUT
Theoretical Study

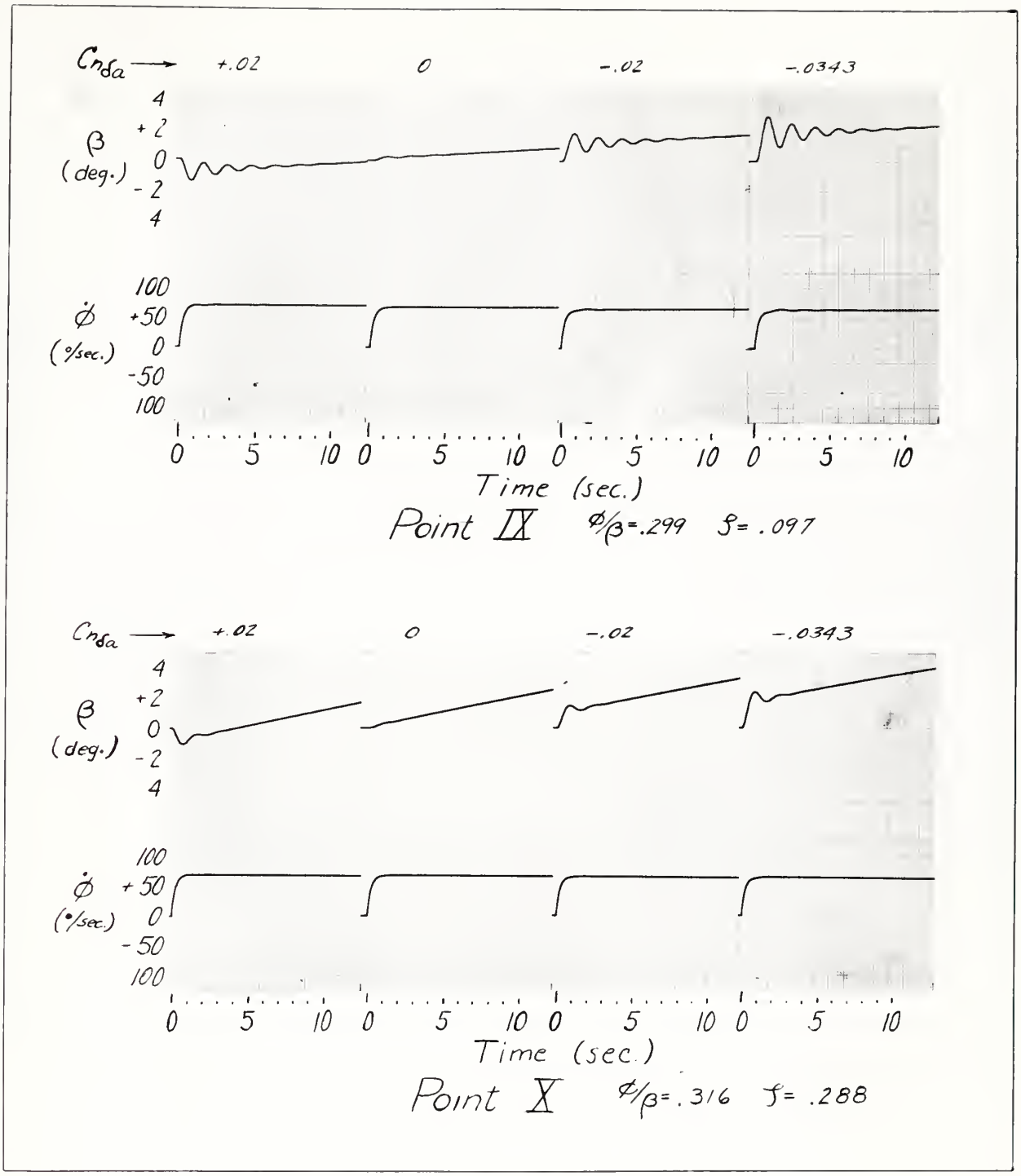

FIGURE 18

ANALOG RESPONSE TO 10° AILERON STEP INPUT
Theoretical Study

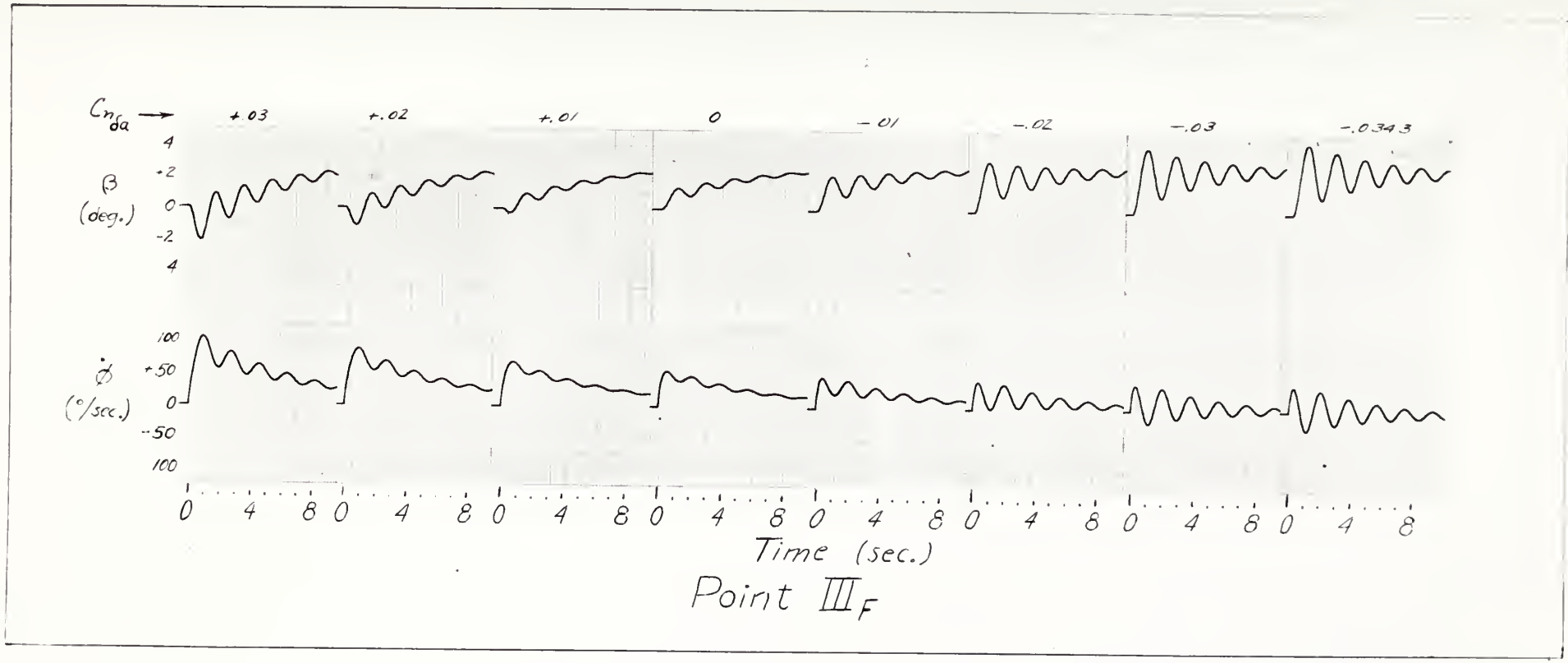

FIGURE 19

ANALOG RESPONSE TO 10° AILERON STEP INPUT
Flight Investigation Points

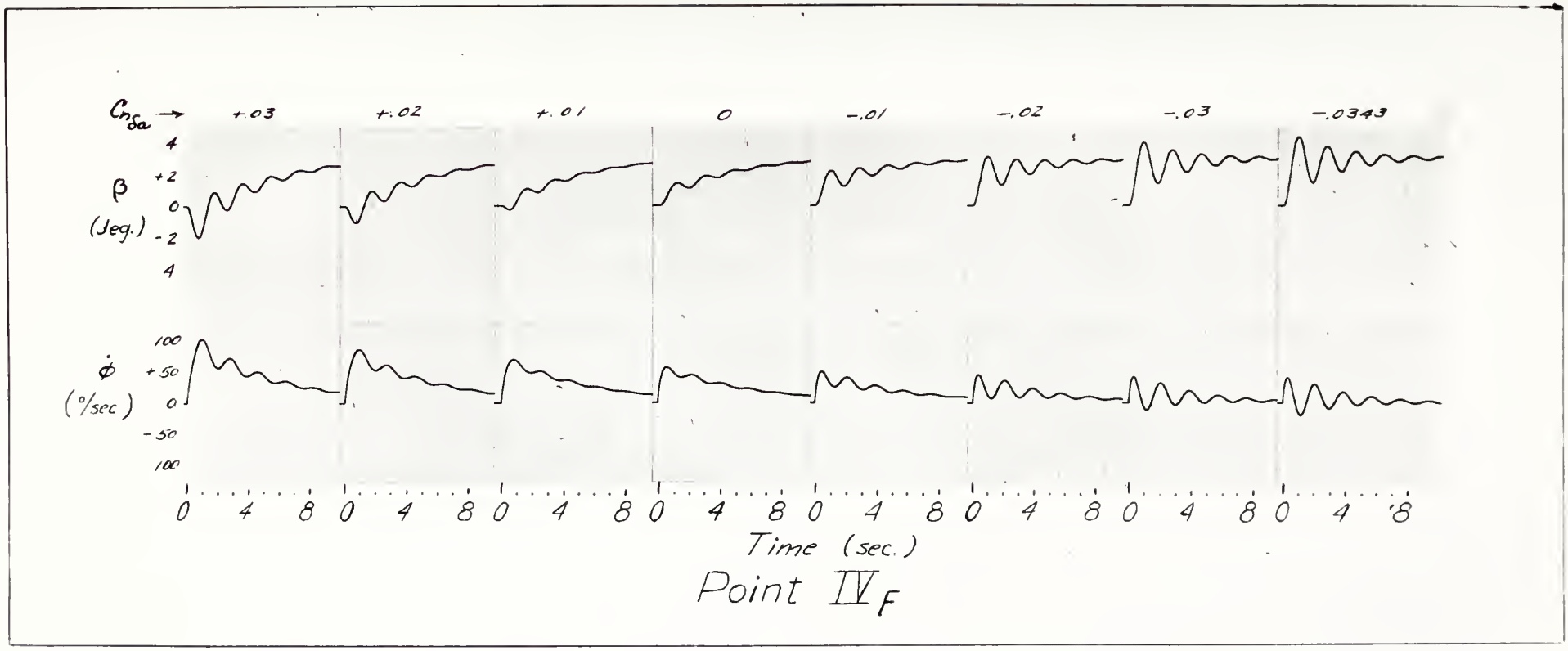

FIGURE 19

ANALOG RESPONSE TO 10° AILERON STEP INPUT
Flight Investigation Points

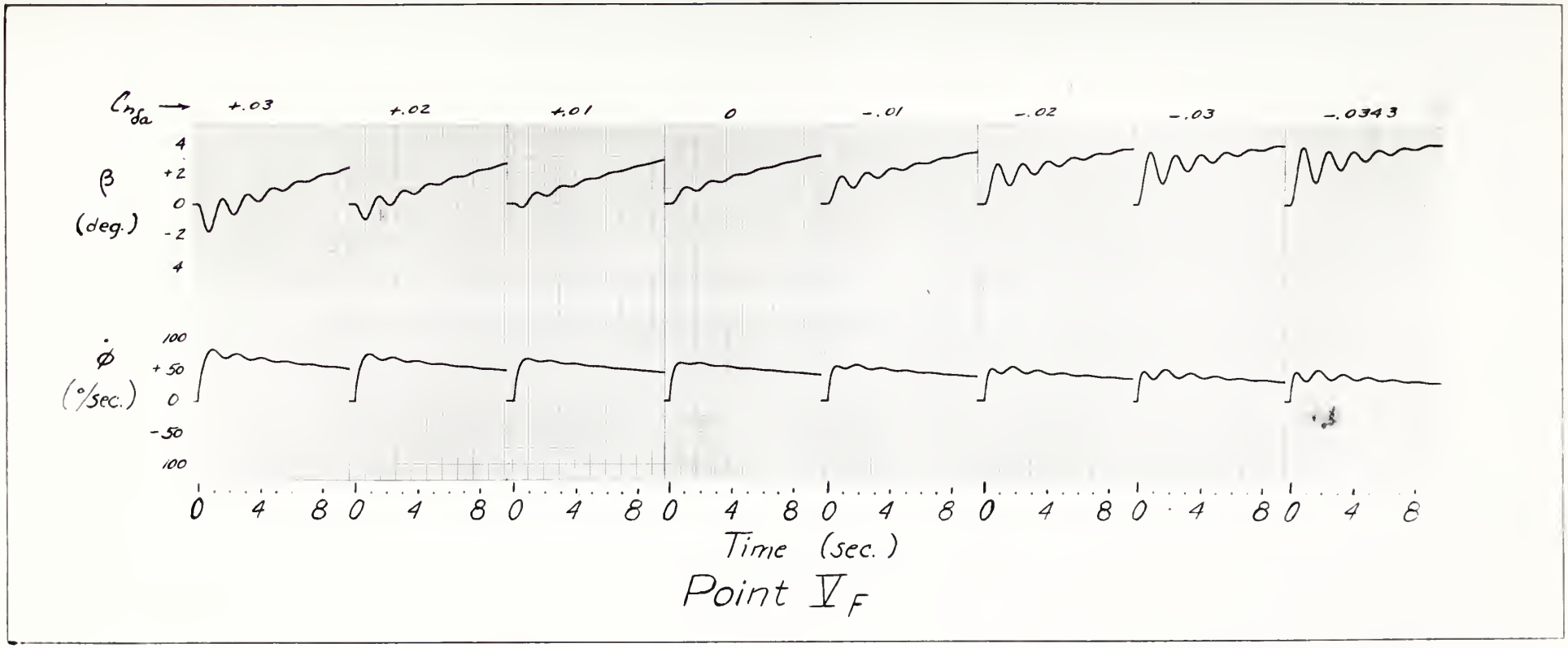

FIGURE 19

ANALOG RESPONSE TO 10° AILERON STEP INPUT
Flight Investigation Points

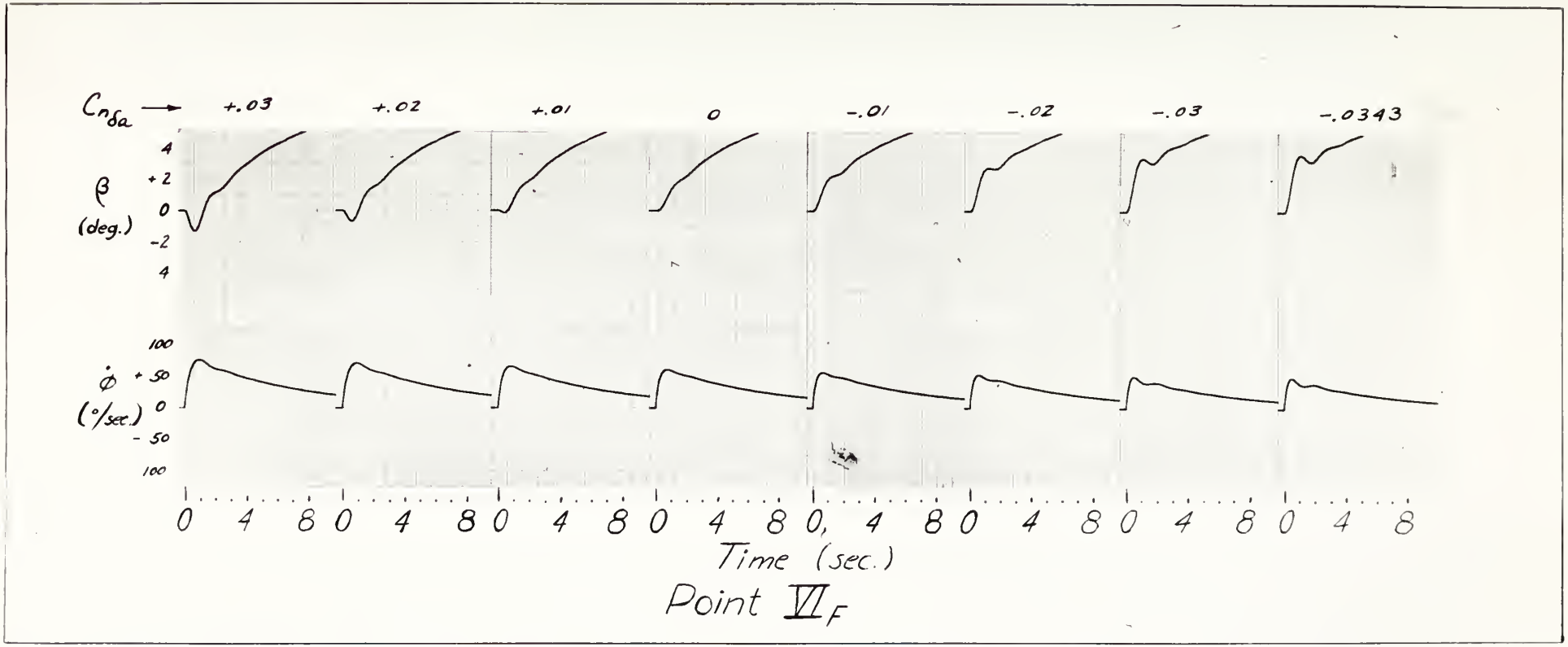

FIGURE 19

ANALOG RESPONSE TO 10° AILERON STEP INPUT
Flight Investigation Points

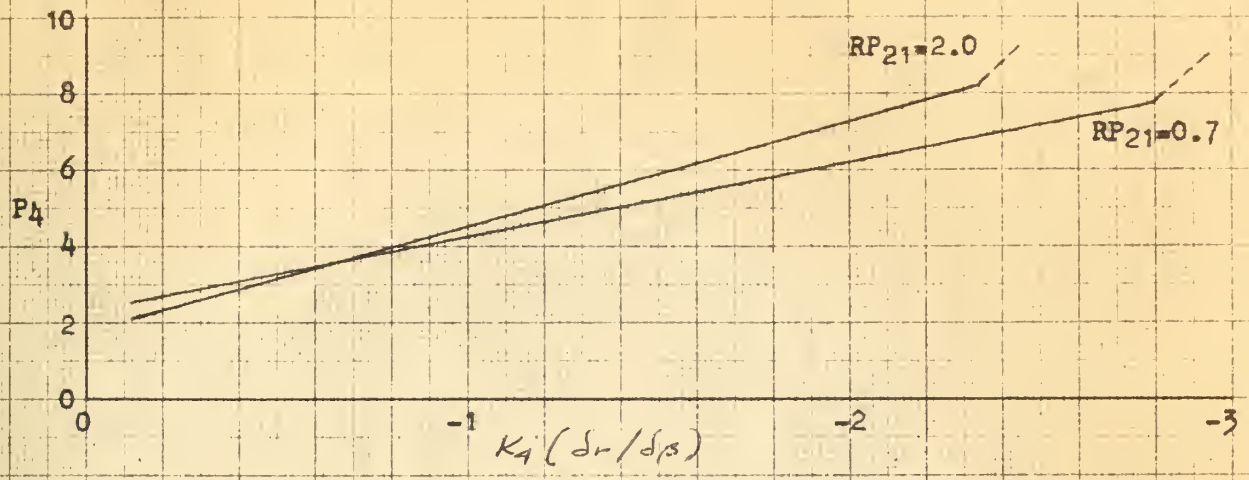

FIGURE 20

K_4 GAIN POTENTIOMETER CALIBRATION
β feedback to yaw channel

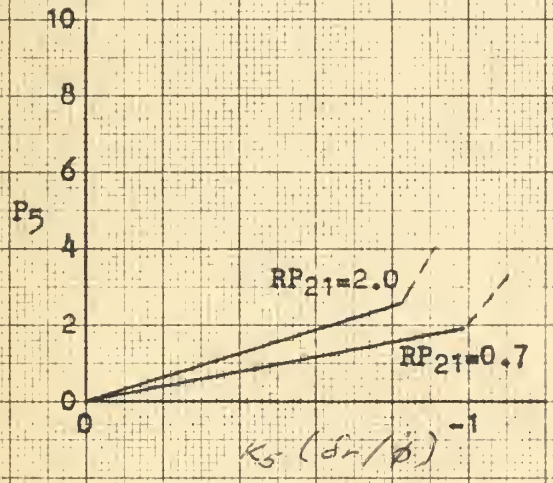

FIGURE 21

K_5 GAIN POTENTIOMETER CALIBRATION
$\dot{\phi}$ feedback to yaw channel
rate gyro #9(28 °/sec max)

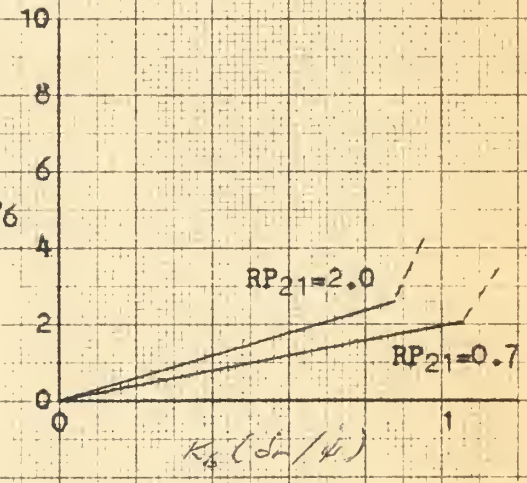

FIGURE 22

K_6 GAIN POTENTIOMETER CALIBRATION
$\dot{\psi}$ feedback to yaw channel, rate gyro #10 (28 °/sec max.)

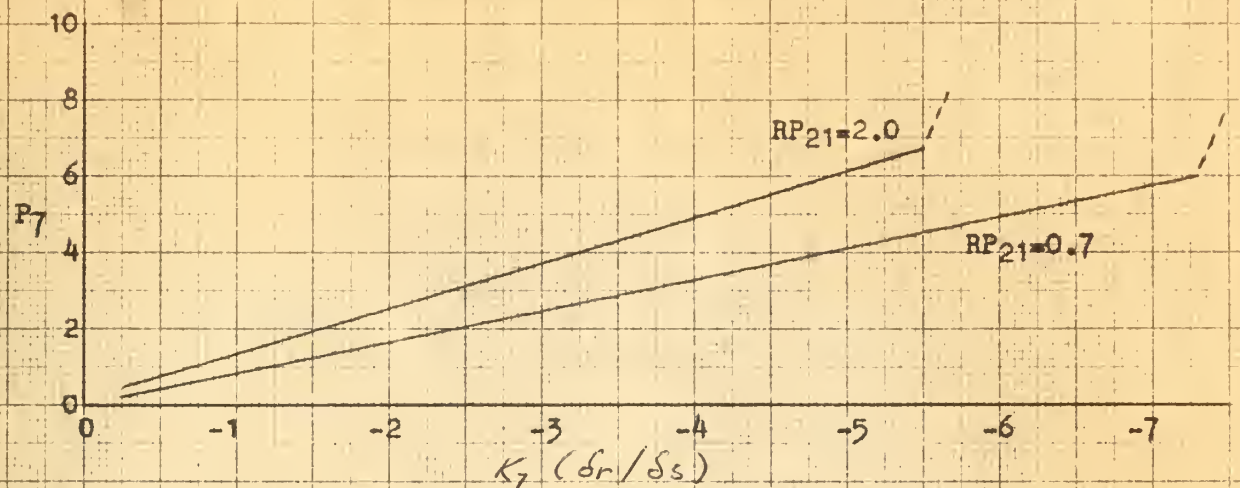

FIGURE 23

K_7 GAIN POTENTIOMETER CALIBRATION
lateral control input to the yaw channel

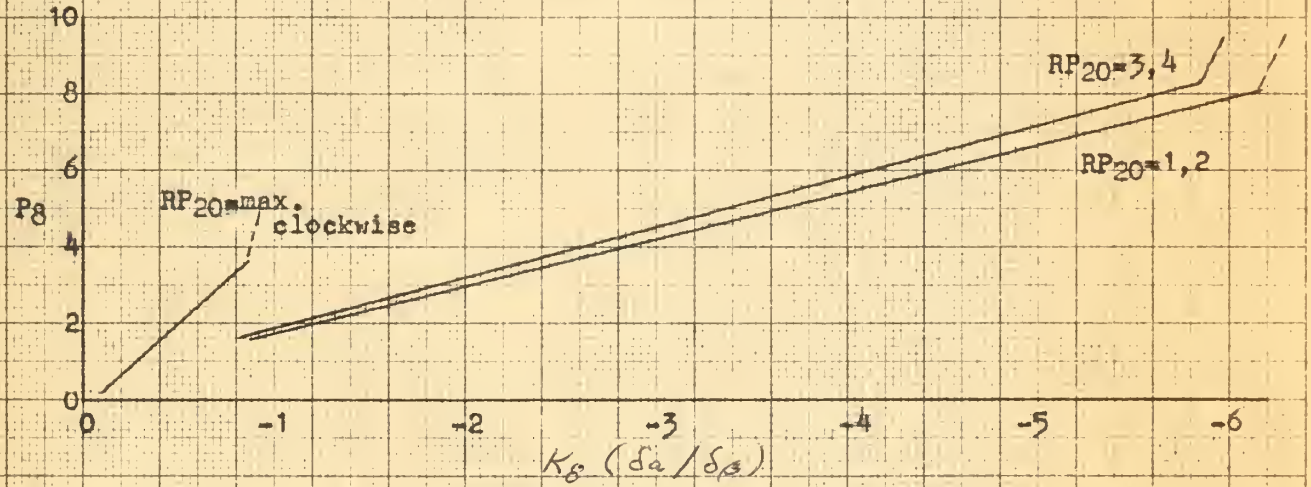

FIGURE 24

K_8 GAIN POTENTIOMETER CALIBRATION
β feedback to roll channel

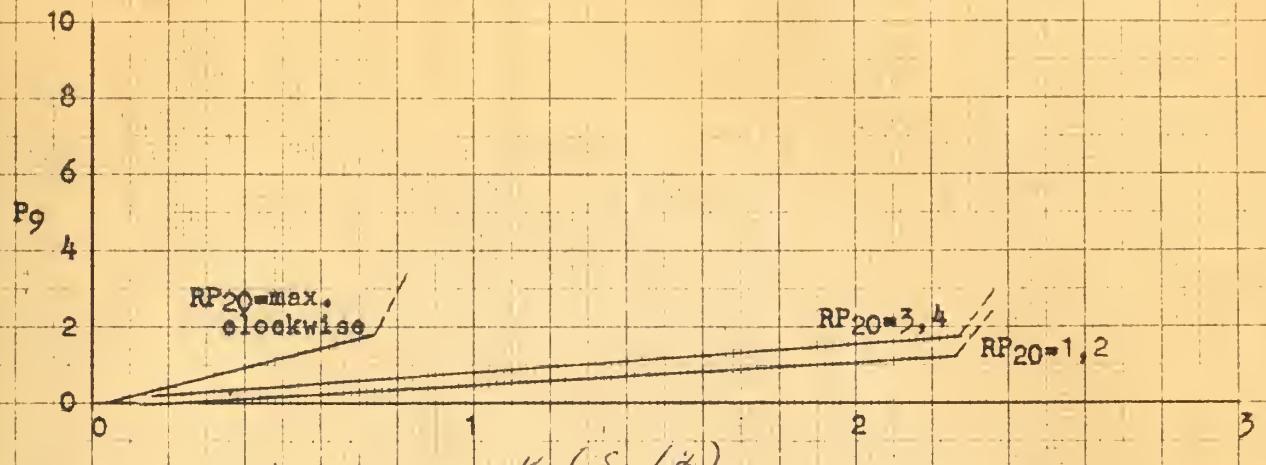

FIGURE 25

K_9 GAIN POTENTIOMETER CALIBRATION
$\ddot{\phi}$ feedback to roll channel
rate gyro #11 (30°/sec max)

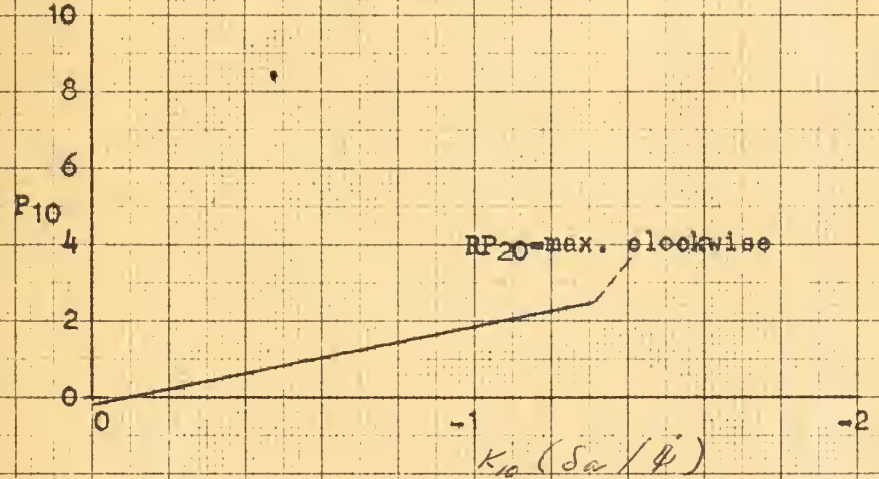

FIGURE 26

K_{10} GAIN POTENTIOMETER CALIBRATION
$\ddot{\phi}$ feedback to roll channel
rate gyro #13 (28°/sec max)

FIGURE 27

$\frac{K_3}{K_1}$ VS. $C_{n_{\delta_a}}$ AT VARIOUS $\frac{\phi}{\beta}$, β_{DR} POINTS

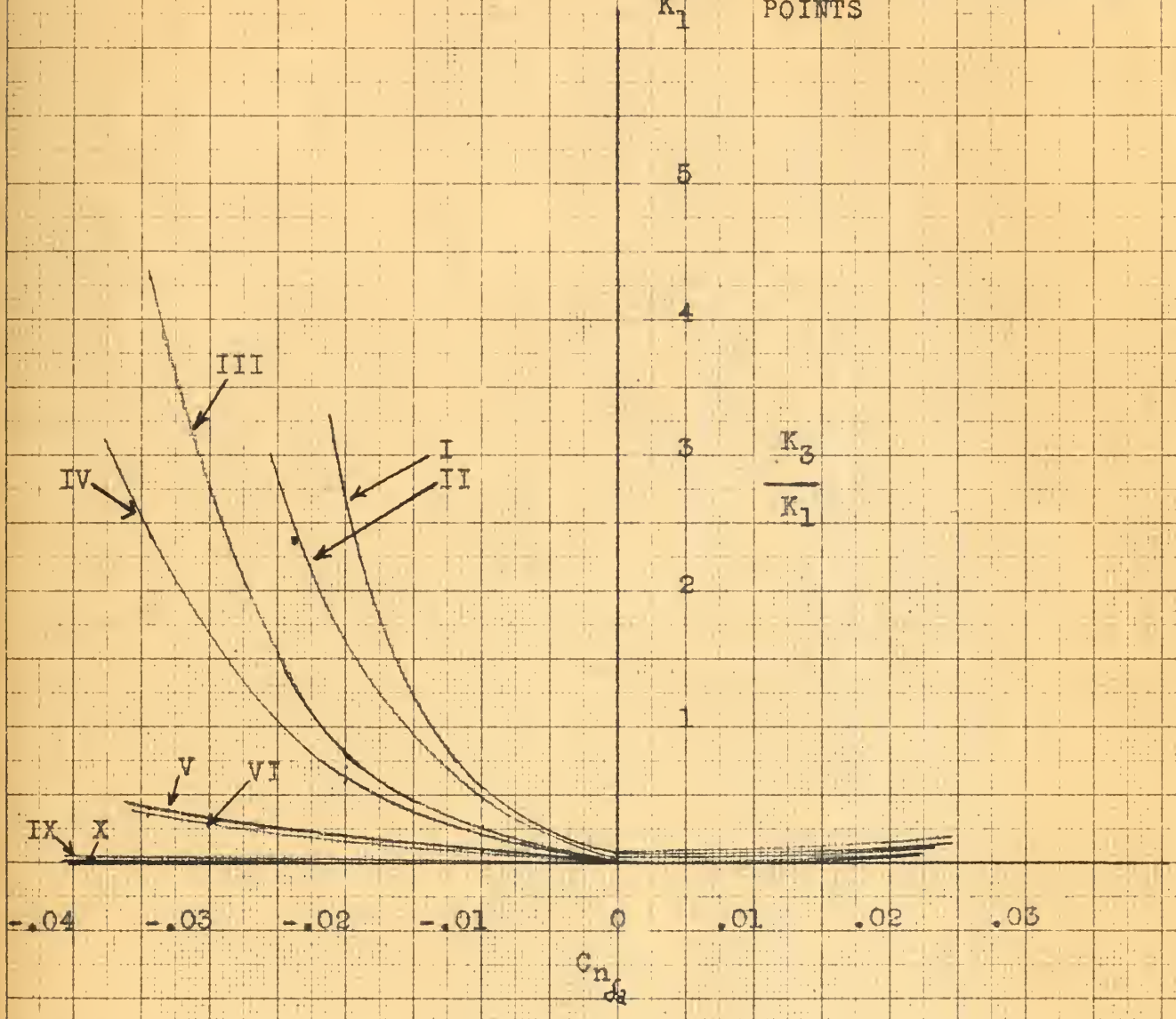

FIGURE 28

$\frac{K_3}{K_1}$ VS. $C_{n_{\delta a}}$ AT VARIOUS β, γ_{DR} FLIGHT POINTS

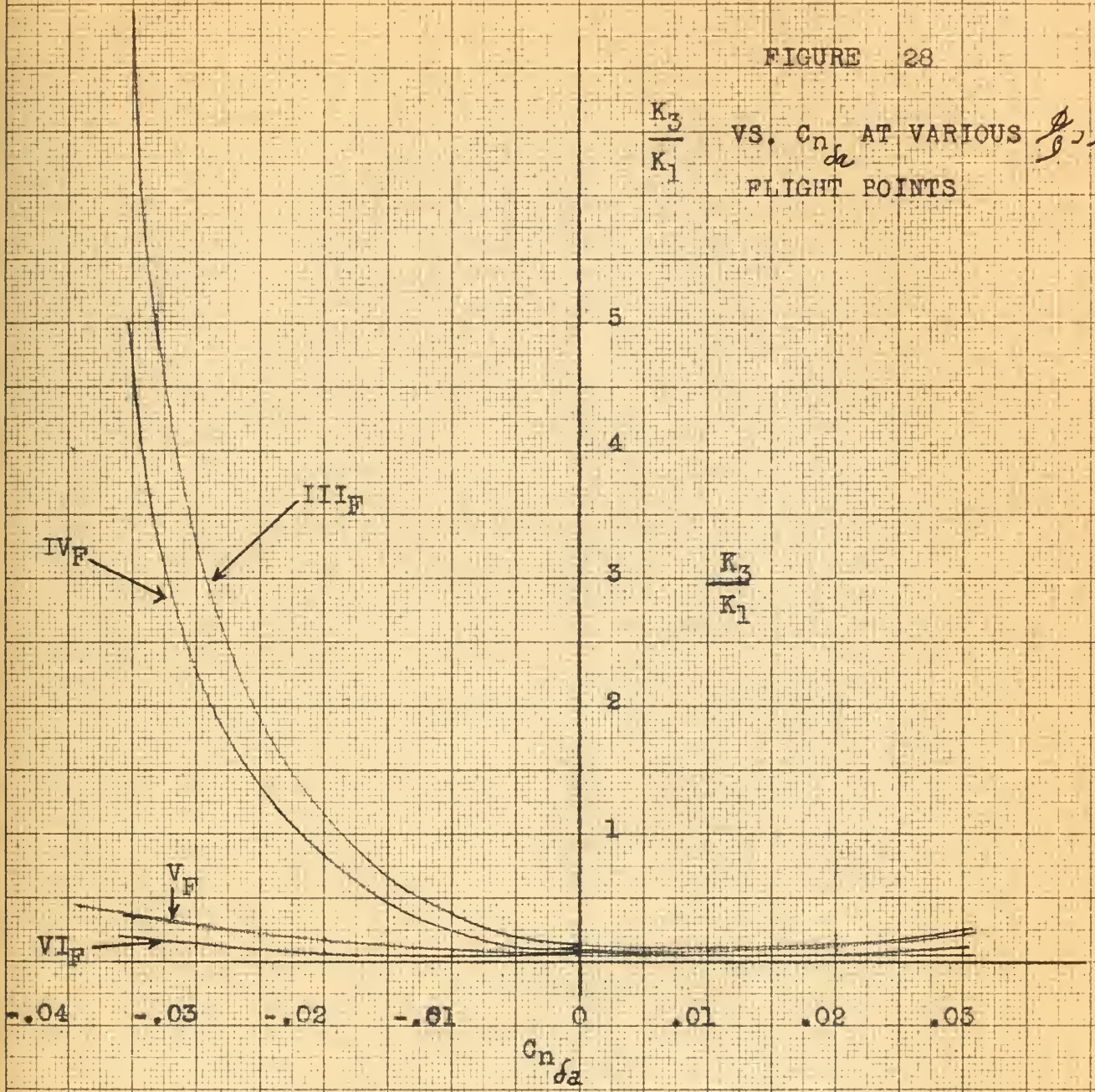

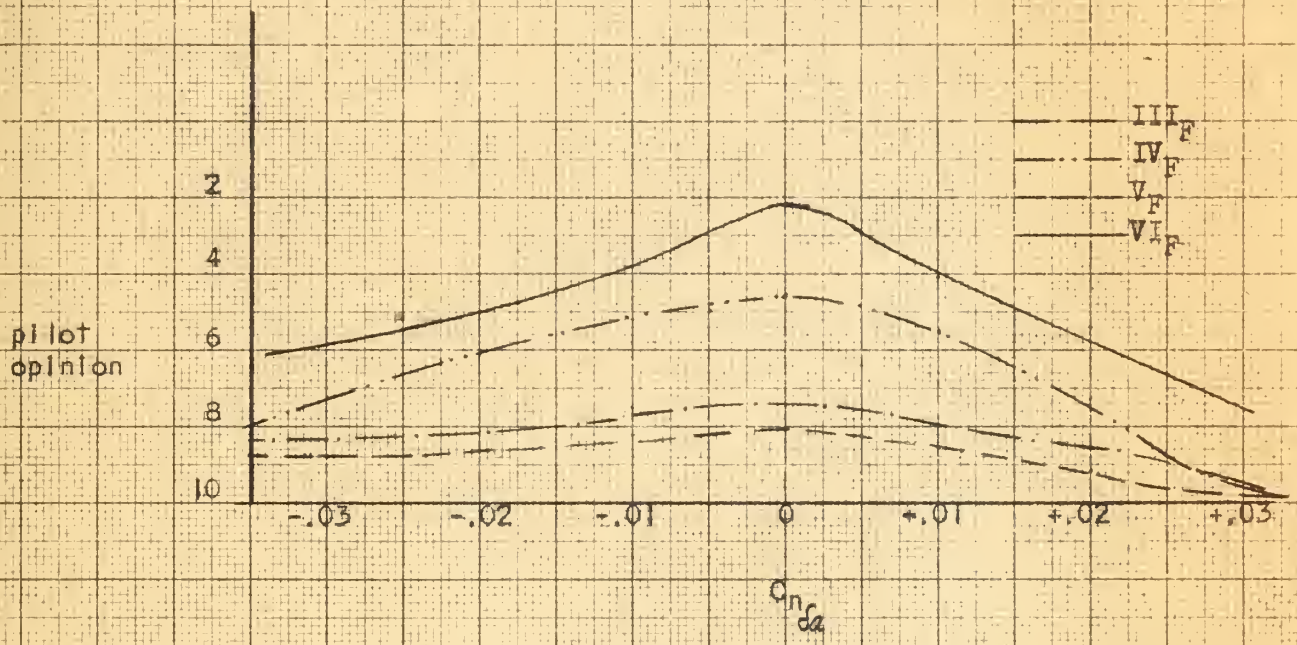

FIGURE 29

PILOT OPINION VS. $C_{n_{\delta a}}$

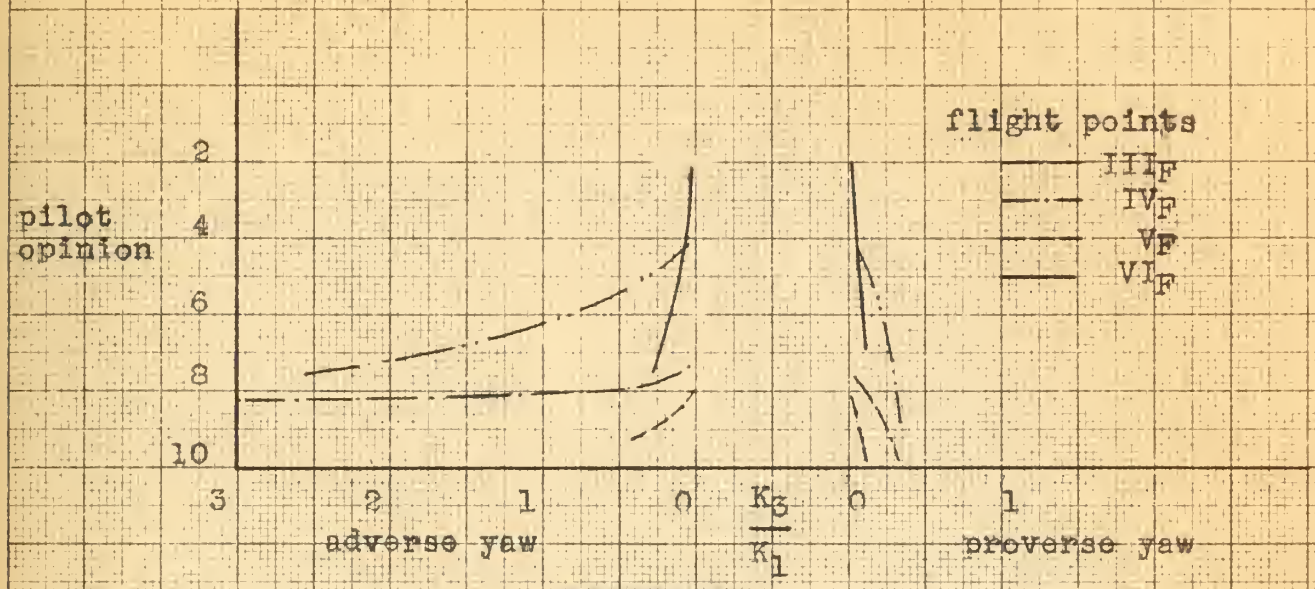

FIGURE 30

PILOT OPINION VS. K_3/K_1 FOR VARIOUS ϕ/β, β_{DR} CONDITIONS

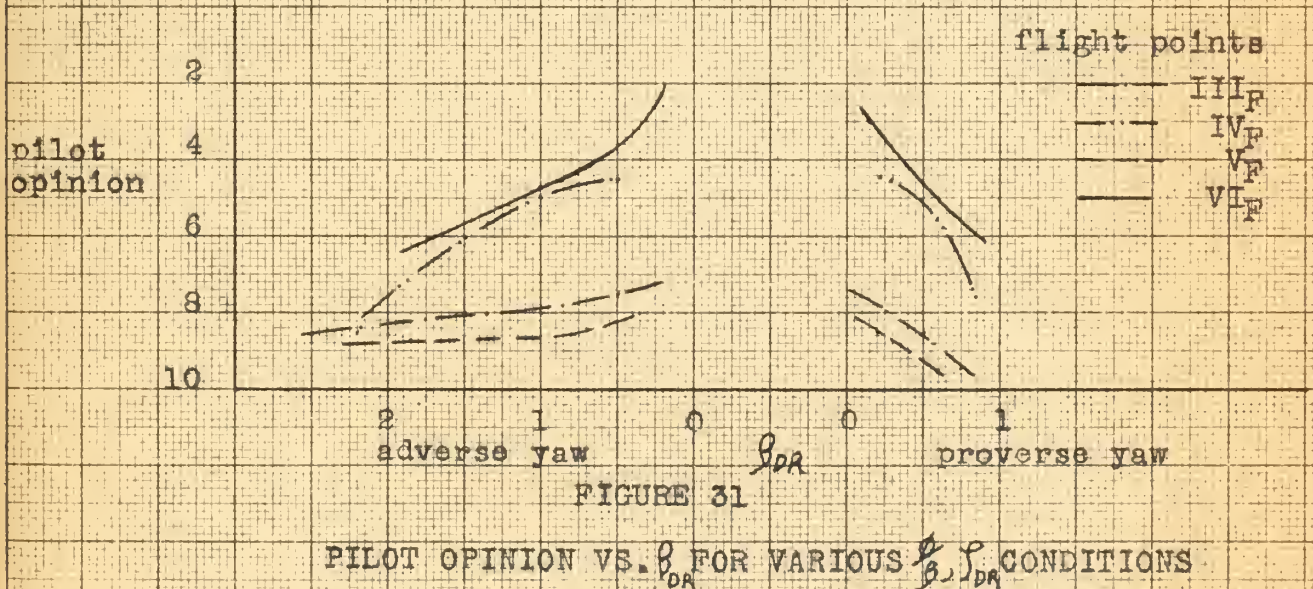

FIGURE 31

PILOT OPINION VS. β_{DR} FOR VARIOUS ϕ/β, β_{DR} CONDITIONS

(β_{DR} corresponds to the β_{DR} envelope value at time zero for a 10° aileron step input)

APPENDIX A

CALCULATIONS IN THE THEORETICAL INVESTIGATION

I. Root loci

In order to determine the effect of varying $C\ell_\beta$, Cn_β, Cn_r and Cn_p upon the the characteristic equation four root loci were constructed.

The lateral equations used, from Reference 5, and considering all products of inertia terms negligible:

$$(Cy_\beta - 2d)\beta - 2d\psi + C_L \phi = 0$$

$$\mu C\ell_\beta \beta + \frac{C\ell_r}{2} d\psi + (\frac{C\ell_p}{2} d - J_x d^2)\phi = - \mu C\ell_{\delta a} \delta a$$

$$\mu Cn_\beta \beta + (\frac{Cn_r}{2} - J_z d)d\psi + \frac{Cn_p}{2} d\phi = - \mu Cn_{\delta a} \delta a$$

Typical values for quantities considering a high performance fighter at m = 1.2 at 35,000 ft.

$Cy_\beta = -.8$

$C_L = .1$

$C\ell_\beta = -.12$

$C\ell_r = +.04$

$C\ell_p = -.4$

$Cn_\beta = +.13$

$Cn_r = -.25$

$Cn_p = -.01$

$\mu = 70$

$I_x = 11{,}000$ slug ft.^{2}

$J_x = .0254$

$I_z = 94{,}000$ slug ft.^{2}

$J_z = .2$

$S = 375$ ft.^{2}

$b = 35.7$

The coefficients of the lateral characteristic equation:

$$AS^4 + BS^3 + CS^2 + DS + E = 0$$

$$A = +1$$

$$B = -1/2\left(Cy_\beta + \frac{Cn_r}{J_z} + \frac{C\ell_p}{J_x}\right)$$

$$C = \frac{1}{4J_x J_z}\left(C\ell_p\, Cn_r - C\ell_r\, Cn_p\right) + \frac{Cy_\beta}{4}\left(\frac{Cn_r}{J_z} + \frac{C\ell_p}{J_x}\right) + \frac{\mu Cn_\beta}{J_z}$$

$$D = \frac{-\mu}{2J_x J_z}\left(Cn_\beta\, C\ell_p - C\ell_\beta\, Cn_p\right) - \frac{\mu}{2J_x} C_L C\ell_\beta - \frac{Cy_\beta}{8J_x J_z}\left(C\ell_p\, Cn_r - C\ell_r\, Cn_p\right)$$

$$E = \frac{\mu C_L}{4J_x J_z}\left(C\ell_\beta\, Cn_r - Cn_\beta\, C\ell_r\right)$$

Solving for the quartic and holding $C\ell_\beta$ as a variable to put the quartic in root locus form

$$S^4 + 9.025S^3 + 53.97S^2 + (366S - 210\, C\ell_\beta)S - 87.5\, C\ell_\beta - 1.8$$

$$1 + \frac{(-210\, C\ell_\beta)(S + .417)}{(S - .005)(S + 8.01)(S + .51 \pm j\, 6.77)} = 0$$

Root locus form with Cn_β as variable:

$$S^4 + 9.025S^3 + (8.47 + 350\, Cn_\beta)S^2 + (2800\, Cn_\beta + 27.2)S + 10.5 - 14\, Cn_\beta = 0$$

$$1 = \frac{(350 Cn_\beta)(S + 8)(S - .005)}{(S + .449)(S + 8.38)(S + .098 \pm j\, 1.728)} = 0$$

Root locus form with Cn_r as variable:

$$S^4 + (8.4 - 2.5\, Cn_r)S^3 + (-21 Cn_r + 48.72)S^2 + (389.2 - 8 Cn_r)S + 42\, Cn_r - 1.82 = 0$$

$$1 = \frac{(-2.5 Cn_r)(S + 8.02)(S + .09 \pm j\, 1.33)}{(S - .00468)(S + 8.23)(S + .0875 \pm j\, 6.88)} = 0$$

Root locus form with Cn_p as the variable:

$$S^4 + 9.025S^3 + (53.95 - 2Cn_p)S^2 + (382.8 - 840.8\, Cn_p)S + 8.68 = 0$$

$$1 + \frac{(-2Cn_p)(S)(S + 420.4)}{(S + .046)(S + 8.15)(S + .426 \pm j\, 6.83)} = 0$$

II. Using the information gained from the above root loci the four variables were changed in an effort to locate ϕ/β from .1 to 10 and ζ from .1 to .3 as shown in Figure 14.

Point I Figure 14.

$Cn_r = -.6$ $\quad Cy_\beta = -.8$ $\quad \mu = 70$

$C\ell_\beta = -.18$ $\quad C_L = .1$ $\quad J_x = .0254$

$Cn_p = -.01$ $\quad C\ell_r = +.04$ $\quad J_z = .2$

$Cn_\beta = .11$ $\quad C\ell_p = -.4$

Characteristic equation:

$$S^4 + 9.9S^3 + 54.32S^2 + 350.615S + 36.26 = 0$$

$$(S + 8.36)(S + .105)(S + .718 \pm j\,6.39) = 0$$

$$\zeta = .111$$

$$\phi/\beta = \frac{2}{C_L - \frac{Cn_p}{J_z}} \quad \frac{S^2 - (\frac{Cn_r}{2J_z} + \frac{Cy_\beta}{2})S + \frac{Cn_r\, Cy_\beta}{4\, J_z} + \frac{\mu Cn_\beta}{J_z}}{S - \frac{Cn_r/2\, J_z}{1 - \frac{Cn_p}{J_z C_L}}}$$

S = dutch roll S

$$\phi/\beta = 8.1$$

Point II Figure 14.

$Cn_r = -1.4$ $\quad Cy_\beta = -.8$ $\quad \mu = 70$

$C\ell_\beta = -.18$ $\quad C_L = .1$ $\quad J_x = .0254$

$Cn_p = -.01$ $\quad C\ell_r = +.04$ $\quad J_z = .2$

$Cn_\beta = +.1$ $\quad C\ell_p = -.4$

Characteristic equation:

$$S^4 + 11.9S^3 + 67.625S^2 + 329S + 86.8 = 0$$

$$(S + 8.37)(S + .279)(S + 1.626 \pm j\,5.88) = 0$$

$$\zeta = .267$$

$$\phi/\beta = 9.52$$

Point III Figure 14.

$Cn_r = -.6$ $\quad Cy_\beta = -.8$ $\quad \mu = 70$

$Cn_p = -.01$ $\quad C_L = .1$ $\quad J_x = .0254$

$Cn_\beta = +.3$ $\quad C\ell_r = .04$ $\quad J_z = .2$

$C\ell_\beta = -.13$ $\quad C\ell_p = -.4$

Characteristic equation:

$$s^4 + 9.9s^3 + 61.32s^3 + 396.1s + 25.48 = 0$$

$$(S + .065)(S + 8.24)(S + .798 \pm J\ 6.85) = 0$$

$$\zeta = .116$$

$$\phi/\beta = 5.3$$

Point IV Figure 14.

$Cn_r = -1.8$ $\quad Cy_\beta = -.8$ $\quad \mu = 70$

$C\ell_\beta = -.12$ $\quad C_L = .1$ $\quad J_x = .0254$

$Cn_\beta = +.13$ $\quad C\ell_r = .04$ $\quad J_z = .2$

$Cn_p = -.01$ $\quad C\ell_p = -.4$

Characteristic equation:

$$s^4 + 12.9s^3 + 86.52s^2 + 403.6s + 73.78 = 0$$

$$(S + 8.21)(S + .191)(S + 2.25 \pm j\ 6.49) = 0$$

$$\zeta = .328$$

$$\phi/\beta = 5.62$$

Point V Figure 14.

$Cn_r = -.6$ $\quad Cy_\beta = -.8$ $\quad \mu = 70$

$Cn_\beta = +.18$ $\quad C_L = .1$ $\quad J_x = .0254$

$C\ell_\beta = -.06$ $\quad C\ell_r = .04$ $\quad J_z = .2$

$Cn_p = -.01$ $\quad C\ell_p = -.4$

Characteristic equation:

$$s^4 + 9.9s^3 + 78.8s^2 + 522.1s + 10.15 = 0$$

$$(S + 8.12)(S + .0194)(S + 881 \pm j\ 7.97) = 0$$

$$\zeta = .11$$

$$\phi/\beta = 1.9$$

Point VI Figure 14.

$Cn_r = -1.8$ $\quad Cy_\beta = -.8$ $\quad \mu = 70$

$C\ell_\beta = -.05$ $\quad C_L = .1$ $\quad J_x = .0254$

$Cn_\beta = +.16$ $\quad C\ell_r = .04$ $\quad J_z = .2$

$Cn_p = -.01$ $\quad C\ell_p = -.4$

Characteristic equation:

$$S^4 + 12.9S^3 + 97.02S^2 + 472.91S + 29.26$$

$$(S + .0619)(S + 8.08)(S + 2.379 \pm j\ 7.22) = 0$$

$\zeta = .31$

$\phi/\beta = 2.0$

Point VII Figure 14.

$Cn_r = -.5$ $\quad Cy_\beta = -.8$ $\quad \mu = 70$

$C\ell_\beta = -.02$ $\quad C_L = .1$ $\quad J_x = .0254$

$Cn_p = -.01$ $\quad C\ell_r = .04$ $\quad J_z = .2$

$Cn_\beta = .2$ $\quad C\ell_p = -.4$

Characteristic equation

$$S^4 + 9.65S^3 + 83.72S^2 + 568.2S + .7 = 0$$

$$(S + 8.03)(S + .0012)(S + .81 \pm j\ 8.37) = 0$$

$\zeta = .096$

$\phi/\beta = .607$

Point VIII Figure 14

$Cn_r = -1.8$ $\quad Cy_\beta = -.8$ $\quad \mu = 70$

$Cn_\beta = +.18$ $\quad C_L = .1$ $\quad J_x = .0254$

$Cn_p = -.01$ $\quad C\ell_r = .04$ $\quad J_z = .2$

$C\ell_\beta = -.02$ $\quad C\ell_p = -.4$

Characteristic equation:

$$S + 12.9S + 104.02S + 522.6S + 10.08 = 0$$

$$(S + .0193)(S + 8.05)(S + 2.416 \pm j\ 7.68)$$

$\zeta = .3$

$\phi/\beta = .711$

Point IX Figure 14

$Cn_r = -.5$ $\quad Cy_\beta = -.8$ $\quad \mu = 70$

$C\ell_\beta = -.01$ $\quad C_L = .1$ $\quad J_X = .0254$

$Cn_p = -.01$ $\quad C\ell_r = .04$ $\quad J_Z = ~~.0254~~ .2$

$Cn_\beta = +.2$ $\quad C\ell_p = -.4$

Characteristic equation:

$$S^4 + 9.65S^3 + 83.7S^2 + 566.1S - 1.05 = 0$$

$$(S - .00185)(S + 8.02)(S + .816 \pm j\ 8.37) = 0$$

$$\zeta = .097$$

$$\phi/\beta = .299$$

Point X Figure 14

$Cn_r = -1.8$ $\quad Cy_\beta = -.8$ $\quad \mu = 70$

$C\ell_\beta = -.01$ $\quad C_L = .1$ $\quad J_X = .0254$

$Cn_p = -.01$ $\quad C\ell_r = .04$ $\quad J_Z = .2$

$Cn_\beta = .2$ $\quad C\ell_p = -.4$

Characteristic equation:

$$S^4 + 12.9S^3 + 111S^2 + 576.51S + 3.5 = 0$$

$$(S + .0061)(S + 8.02)(S + 2.437 \pm j\ 8.12)$$

$$\zeta = .288$$

$$\phi/\beta = .316$$

APPENDIX B

ANALOG COMPUTER COMPUTATIONS

The objectives of the analog study were to verify and expand the results of the theoretical investigation, Appendix A (i.e., to observe the roll rate response to a step aileron input for various values of the airplane's stability derivatives, namely $C\ell_\beta$, Cn_r, Cn_β and $Cn_{\delta a}$).

The non-dimensional, linearized lateral perturbation equations of motion (Reference 5) are:

$$(Cy_\beta - 2d)\beta - 2d\psi + C_L\phi = 0$$

$$\mu\, C\ell_\beta\beta + \frac{C\ell_r}{2} d\psi + \left(\frac{C\ell_p}{2} d - J_x d^2\right)\phi = - \mu\, C\ell_{\delta a}\, \delta a$$

$$\mu\, Cn_\beta\beta + \left(\frac{Cn_r}{2} d - J_z d^2\right)\psi + \frac{Cn_p}{2} d\phi = - \mu\, Cn_{\delta a}\, \delta a$$

These equations represent the sideforces, rolling moments and yawing moments, respectively. The d and d^2 terms are with respect to non-dimensional time, t/τ. The derivative subscripts p and r represent the non-dimensional helix angles pb/2V and rb/2V. The initial conditions for the equations of motion are steady, wings-level horizontal flight. The excitation for the analog computer evaluations was a unit step aileron input (δa).

Except for the variable derivatives previously mentioned, all other derivative values are typical of a high performance airplane at Mach 1.2 and 35,000 feet. Typical derivatives as obtained from NASA reports are:

$Cy_\beta = - 0.8$	$C\ell_r = + 0.04$	$Cn_r = - 0.25$
$C_L = + 0.1$	$Cn_p = - 0.01$	$C\ell_p = - 0.4$
$C\ell_\beta = - 0.12$	$Cn_\beta = + 0.13$	$C\ell_{\delta a} = + 0.04$
$J_x = 0.025$	$J_z = 0.2$	$\mu = 70$

The equations of motion become:

$$(-0.8 - 2d)\beta + (-2d)\dot{\psi} + 0.1\phi = 0$$

$$70\, C\ell_\beta \beta + (0.02d)\dot{\psi} + (-0.2d - 0.025d^2)\phi = -2.8\, \delta a$$

$$70\, Cn_\beta \beta + \left(\frac{Cn_r}{2} d - 0.2\, d^2\right)\dot{\psi} + (-0.005\, d)\phi = -70\, Cn_{\delta a}\delta a$$

An analog computer board was set up as described in Figure 16. The summing points in the three rows of amplifiers in Figure 17 are for the rolling moment, yawing moment, and sideforce equations, in order. The terms in the equations of motion represent current (μ amps) flow into the summing points on the analog diagram. For example, the $\ddot{\phi}$ term in the rolling moment equation above is $-0.025\ddot{\phi}$ μ amps. The output of amplifier 1 is arbitrarily selected to be $-0.2\ddot{\phi}$ volts. R_{f_1} is arbitrarily selected to be 5 megohms. The P_1 potentiometer setting is calculated as follows:

$$\frac{(P_1)\,(-0.2\ddot{\phi})\ \text{volts}}{(R_{f_1})\ \text{megohms}} = -0.025\ddot{\phi}$$

$$\frac{P_1(-0.2)}{5} = -0.025$$

$$P_1 = 0.625$$

If P_1 is calculated to be greater than its limiting value of 1.0, R_{f_1} must be changed accordingly.

To determine the δa step inputs to the analog circuit, it was necessary to reduce the standard 200 volt computer input as follows:

Let 5 volts or amps = 1 physical unit

ϕ, β, ψ, δa in radians

$\dot{\phi}$, $\dot{\psi}$ in radians/airsec

$$\mu C\ell_{\delta a}\, \delta a = (70)\,(+.04)\,(5) = 14\ \mu \text{ amps}$$

To reduce 200 volts to get 14 μ amps current, two potentiometers (P_A and P_B, Figure 17) reduced the voltage to 14 volts, which was put across a 1 megohm resistance (R_B, Figure 17) to get the $\mu C\ell_{\delta a}\, \delta a$ input.

$I = E/R = 14$ volts/1 megohm = 14 μ amps

$\mu\ Cn_{\zeta a}\ \zeta a = (70)\ (Cn_{\delta a})\ (5) = 350\ Cn_{\delta a}$

$Cn_{\delta a}$ (derivative)	350 $Cn_{\zeta a}$ (μamps)
0	0
$\pm$ 0.01	$\pm$ 3.5
$\pm$ 0.02	$\pm$ 7.0
$\pm$ 0.03	$\pm$ 10.5
$\pm$ 0.0343	$\pm$ 12.0

Potentiometers P_C and P_D, Figure 17, reduced the 200 volt input to the desired voltage which was then put across a 1 megohm resistance to obtain the desired $Cn_{\zeta a}$ current values. The analog recordings for test points I through X of the theoretical investigation are illustrated in Figure 18.

APPENDIX C

DIMENSIONAL EQUATIONS OF MOTION

The airplane equations of motion were dimensionalized in the following manner to apply them to the autopilot:

Airplane equations:

$$(Cy_\beta - 2d)\beta - 2d\,\dot{\psi} + C_L\phi = 0$$

$$\mu C\ell_\beta\,\beta + \frac{C\ell_r}{2}\,d\,\dot{\psi} + \left(\frac{C\ell_p}{2}\,d - J_x\,d^2\right)\phi = -\mu C\ell_{\delta a}\,\delta a$$

$$\mu Cn_\beta\,\beta + \left(\frac{Cn_r}{2} - J_z d\right)d\dot{\psi} + \frac{Cn_p}{2}\,d\phi = -\mu Cn_{\delta a}\,\delta a$$

Putting the equations in real time

$$\left(\frac{Cy_\beta}{2\tau} - S\right)\beta + \dot{\psi} + \frac{C_L}{2\tau}\,\phi = 0$$

$$\frac{\mu C\ell_\beta}{J_x 2\tau}\,\beta + \frac{C\ell_r}{2J_x\tau}\,\dot{\psi} + \left(\frac{C\ell_p}{2J_x\,\tau}\,S - S^2\right)\phi = -\frac{\mu C\ell_{\delta a}}{J_x\,\tau^2}\,\delta a$$

$$\frac{\mu Cn_\beta}{J_x\,\tau^2}\,\beta + \left(\frac{Cn_r}{2J_z\tau} - S\right)\dot{\psi} + \frac{Cn_p}{2J_z\tau}\,\phi = -\frac{\mu Cn_{\delta a}}{J_z\,\tau^2}\,\delta a$$

$$J_x = 2\left(\frac{K_x}{b}\right)^2 \qquad J_z = 2\left(\frac{K_z}{b}\right)^2 \qquad \mu = \frac{m}{\rho S b} \qquad \tau = \frac{m}{\rho S V_o}$$

$$(Y_v - S)\beta - \dot{\psi} + \frac{g}{V_o}\,\phi = 0$$

$$L_\beta\,\beta + L_r\,\dot{\psi} + (L_p\,S - S^2)\phi = -L_{\delta a}\,\delta a$$

$$N_\beta\,\beta + (N_r - S)\,\dot{\psi} + N_p\,S\phi = -N_{\delta a}\,\delta a$$

The defining equations for converting NAvion dimensional derivatives to derivatives of the aircraft being simulated by means of the autopilot are listed in Table V.

APPENDIX D

C_{n_r} CORRECTION FOR β VANE LOCATION

The sideslip vane location ahead of the center of gravity produces a destabilizing effect on the rudder which is caused by the yaw rate r, acting on the β vane. It was considered desirable to determine the magnitude of this reduction in C_{n_r} since the dutch roll appeared to be neutrally damped in the airplane when theoretically, without giving consideration of vane displacement from the c.g. positive damping was expected.

x = distance from c.g forward to β vane $\approx$ 4'

y = distance from c.g. out the y axis to the β vane.

$\Delta\beta$ due to yawing velocity = $\frac{rx}{V}$

ΔC_n due to yawing velocity = $Cn_{\delta r} \frac{\delta r}{\delta \beta} \Delta\beta$

$$\Delta Cn_r = \frac{\Delta Cn}{\frac{rb}{2V}} = Cn_{\delta r} \frac{\delta r}{\delta \beta} \frac{\frac{rx}{V}}{\frac{rb}{2V}} = Cn_{\delta r} \frac{\delta r}{\delta \beta} \frac{2x}{b}$$

Flight Points V_F and VI_F where low ζ's were observed are used to determine the ΔC_{n_r} reduction

For both III_F and IV_F $\Delta C_{n_r} = - .0691 (- 2.12) \frac{8}{16} = + .0734$

$$\Delta Nr = .0874$$

Point V_F $\frac{\Delta Nr}{Nr} = \frac{.0874}{.714} = 12\%$

Point VI_F $\frac{\Delta Nr}{Nr} = \frac{.0874}{2.14} = 4\%$

The values of K_6 and K_{10} must be changed in order to remove the effect from the aircraft. Point V_F is illustrated below as an example, for this is where the highest value of ΔNr reduction has been found to prevail.

$K_6 = - .124 - .002415\ L''_r - .2775\ N''_r$

$K_{10} = - .0828 + .049\ L''_{\delta r} + .0278\ N''_r$

The amount that N''_r is reduced by yawing velocity is added to the value of N''_r desired, in order that the yawing velocity effect be eliminated.

Now $K_6 = + .098$ Prior to this correction $K_6 = + .074$

$K_{10} = - .0864$ $K_{10} = - .084$